

~~CONFIDENTIAL~~

Copy 260  
RM L50J27

NACA RM L50J27

TECH LIBRARY KAFB, NM  
0143755

~~CONFIDENTIAL~~  
NACA <sup>ORR</sup> TECHNICAL LIBRARY  
AFL 2291

# RESEARCH MEMORANDUM

STABILITY AND CONTROL CHARACTERISTICS OF  
A  $\frac{1}{4}$ -SCALE BELL X-5 AIRPLANE MODEL  
IN THE LANDING CONFIGURATION

By Robert E. Becht

Langley Aeronautical Laboratory  
Langley Air Force Base, Va.

CLASSIFICATION CHANGED TO UNCLASSIFIED

AUTHORITY J.W. GROWLEY Oct. 29, 1951

CHANGE #2815 WEL

CLASSIFIED DOCUMENT

This document contains classified information affecting the National Defense of the United States within the meaning of the Espionage Act, USC 50,51 and 52. Its transmission or the revelation of its contents in any manner to an unauthorized person is prohibited by law.  
Information so classified may be imparted only to persons in the military and naval services of the United States, appropriate civilian officers and employees of the Federal Government who have a legitimate interest therein, and to United States citizens of known loyalty and discretion who of necessity must be informed thereof.

NATIONAL ADVISORY COMMITTEE  
FOR AERONAUTICS  
WASHINGTON

December 18, 1950

~~CONFIDENTIAL~~

7219



## NATIONAL ADVISORY COMMITTEE FOR AERONAUTICS

## RESEARCH MEMORANDUM

## STABILITY AND CONTROL CHARACTERISTICS OF

A  $\frac{1}{4}$ -SCALE BELL X-5 AIRPLANE MODEL

## IN THE LANDING CONFIGURATION

By Robert E. Becht

## SUMMARY

An investigation was made of the static stability and control characteristics of a  $\frac{1}{4}$ -scale model of a preliminary Bell X-5 airplane design in the landing configuration with and without dive brakes. The changes in trim produced in going from the clean to the landing configuration would necessitate the use of a compensating elevator deflection of about  $-5.7^\circ$ . Adequate elevator effectiveness was available to trim to the maximum lift coefficients attainable in the landing configuration. The use of plug-type fuselage dive brakes caused an unstable stall, but this condition could be corrected by use of a small wing spoiler. On the other hand, flap-type fuselage dive brakes produced a stable stall, and also a general reduction in longitudinal stability over the lift-coefficient range with slight instability at the intermediate lift coefficients of both  $20^\circ$  and  $60^\circ$  wing sweep angles.

## INTRODUCTION

An investigation of the static stability and control characteristics at low speed of a  $\frac{1}{4}$ -scale model of a preliminary Bell X-5 airplane design has been conducted in the Langley 300 MPH 7- by 10-foot tunnel. The Bell X-5 airplane is a proposed research airplane whose sweepback angle can be varied continuously between  $20^\circ$  and  $60^\circ$ . Provision for longitudinal translation of the wing with respect to the fuselage is also made.

The results of the previous investigations of the stability and control characteristics of the Bell X-5 airplane model at low speed are presented in references 1 to 3. The present paper contains the results

of an investigation of the stability and control characteristics of the model in the landing configuration with dive brakes retracted and extended. The results of exploratory tests made to determine the effect of leakage through the fuselage at the wing root are also included.

## SYMBOLS

The system of axes employed, together with an indication of the positive forces, moments, and angles, is presented in figure 1.

$C_L$	lift coefficient ( $Lift/qS$ )
$C_X$	longitudinal-force coefficient ( $X/qS$ )
$C_Y$	lateral-force coefficient ( $Y/qS$ )
$C_L$	rolling-moment coefficient ( $L/qSb$ )
$C_m$	pitching-moment coefficient ( $M/qSc_{50}$ )
$C_n$	yawing-moment coefficient ( $N/qSb$ )
$X$	longitudinal force along X-axis, pounds
$Y$	lateral force along Y-axis, pounds
$Z$	force along Z-axis, pounds ( $Lift = -Z$ )
$L$	rolling moment about X-axis, foot-pounds
$M$	pitching moment about Y-axis, foot-pounds
$N$	yawing moment about Z-axis, foot-pounds
$q$	free-stream dynamic pressure, pounds per square foot ( $\rho V^2/2$ )
$S$	wing area, square feet
$\bar{c}$	wing mean aerodynamic chord (based on plan forms shown in fig. 2), feet
$\bar{c}_{50}$	mean aerodynamic chord at $50^\circ$ sweep, feet
$c'$	streamwise wing chord, feet
$c$	wing chord perpendicular to quarter-chord line of unswept wing, feet

b	wing span, feet
V	free-stream velocity, feet per second
A	aspect ratio ( $b^2/S$ )
$\rho$	mass density of air, slugs per cubic foot
$\alpha$	angle of attack of thrust line, degrees
$\psi$	angle of yaw, degrees
$i_t$	angle of incidence of stabilizer with respect to thrust line, degrees
$\delta$	control-surface deflection measured in a plane perpendicular to hinge line, degrees
$\Lambda$	angle of sweepback of quarter-chord line of unswept wing, degrees

## Subscripts:

e	elevator
f	flap
$\psi$	denotes partial derivative of a coefficient with respect to yaw (example: $C_{L\psi} = \frac{\partial C_L}{\partial \psi}$ )

## APPARATUS AND METHODS

## Description of Model

The model used in this investigation was a  $\frac{1}{4}$ -scale model of a preliminary Bell X-5 airplane design and must, therefore, be considered only qualitatively representative of the Bell X-5 airplane.

Physical characteristics of the basic model are presented in figure 2 and photographs of the model on the support strut are given in figure 3. Figure 4 presents the details of the landing gears and doors and figure 5, the details of the flaps and slats as used in this investigation. The details of the plug-type and the flap-type fuselage dive brakes are given in figure 6 along with a sketch of the gap at the wing

root. Details of the wing spoiler as used in this investigation are also given in this figure.

The wings were pivoted about axes normal to the wing chord planes. The wing incidence measured in a streamwise direction was zero for all sweep angles. At all sweep angles, the wing was located so the quarter chord of the mean aerodynamic chord fell at a fixed fuselage station. The moment reference center was located at this same fuselage station. (See fig. 2.)

The jet-engine ducting was simulated on the model by the use of an open tube having an inside diameter equal to that of the jet exit and extending from the nose to the jet exit.

### Tests

The tests were conducted in the Langley 300 MPH 7- by 10-foot tunnel at a dynamic pressure of 34.15 pounds per square foot which corresponds to a Mach number of 0.152 and a Reynolds number of  $2 \times 10^6$  based on the mean aerodynamic chord of the wing at  $50^\circ$  sweep for average test conditions.

During the tests, no control was imposed on the flow quantity through the jet duct. Measurements of the flow quantity indicated that the inlet-velocity ratio varied between 0.78 and 0.86, the higher values being observed at low angles of attack.

Longitudinal tests were made through the angle-of-attack range by utilizing three tail configurations, tail off and tail incidences of  $-3\frac{3}{4}^\circ$  and  $-5^\circ$ .

Two types of tests were employed for determining the lateral characteristics of the model. The parameters,  $C_{n_\psi}$ ,  $C_{Y_\psi}$ , and  $C_{l_\psi}$  were determined from tests through the angle-of-attack range at yaw angles of  $0^\circ$  and  $5^\circ$ . The lateral characteristics were also determined from tests through a range of yaw angles at constant angle of attack.

### Corrections

The angle-of-attack, drag, and pitching-moment results have been corrected for jet-boundary effects computed on the basis of unswept wings by the methods of reference 4. Independent calculations have shown that the effects of sweep on these corrections are negligible. All coefficients have been corrected for blocking by the model and its wake by the method of reference 5.

Corrections for the tare forces and moments produced by the support strut have not been applied. It is probable, however, that the significant tare corrections would be limited to small increments in pitching moment and drag.

Vertical buoyancy on the support strut, tunnel air-flow misalignment and longitudinal-pressure gradient have been accounted for in computation of the test data.

## RESULTS AND DISCUSSION

### Presentation of Results

The longitudinal aerodynamic characteristics of the model with 20° wing sweep having both slats and flaps retracted and extended are presented in figures 7 and 8, respectively. These data were obtained from retests of the model to allow for comparison with the aerodynamic characteristics of the model in the various configurations to follow. The original data for these configurations, as given in references 1 and 3, were not used inasmuch as the wing of the test model was refinished at the conclusion of the investigation reported in reference 3. Close agreement, however, was obtained with the data presented in reference 3 and reference 1 for the same model configurations.

The principal results of the investigation are presented as follows:

	Figures
Effect of landing gear and gear doors:	
Longitudinal characteristics . . . . .	9 to 12
Longitudinal control . . . . .	13
Lateral and directional characteristics . . . . .	14
Effect of dive brakes:	
Longitudinal characteristics . . . . .	15 to 19
Lateral and directional characteristics . . . . .	20
Effect of air gap around wing root:	
Longitudinal characteristics . . . . .	21
Lateral and directional characteristics . . . . .	22

The aerodynamic coefficients presented herein are based on the wing area and span of the sweep configuration in question and on the mean aerodynamic chord of the wing at 50° sweep. Thus, the pitching-moment coefficients are based on a reference length which is fixed with respect to the fuselage and is independent of sweep angle, whereas all other coefficients are of the usual form.

The Effect of Slats, Flaps, Landing Gear, and Gear Doors

Characteristics in pitch.- In order to provide an index of the change in stability, the change in trim, and the change in drag coefficient produced by the various modifications, the parameters,  $\frac{\partial C_m}{\partial C_L}$ ,  $C_m$ , and  $C_x$  have been evaluated at a lift coefficient of 0.6 and are tabulated in the following table. The elevator deflection required to trim the model at  $C_L = 0.6$  with a  $-\frac{3}{4}^\circ$  tail setting is also included. The lift coefficient of 0.6 was chosen as the value at which flaps, slats, and landing gear might be extended.

Configuration	$\frac{\partial C_m}{\partial C_L}$ (tail off)	$\frac{\partial C_m}{\partial C_L}$ ( $i_t = -\frac{3}{4}$ )	$\frac{\partial C_m}{\partial C_L}$ ( $i_t = -5$ )	$C_m$ ( $i_t = -\frac{3}{4}$ )	$C_x$ ( $i_t = -\frac{3}{4}$ )	$\delta_{e_{trim}}$
Clean	0.024	-0.063	-0.068	-0.042	-0.044	-4.5
Slats and flaps extended	0.033	-0.059	-0.093	-0.082	-0.123	-----
Gear down and doors on	0.019	-0.042	-0.047	-0.048	-0.077	-----
Gear down and doors off	0.035	-0.063	-0.073	-0.052	-0.077	-----
Slats and flaps extended, gear down and doors on (landing configuration)	0.028	-0.066	-0.071	-0.084	-0.160	-10.2
Slats and flaps extended, gear down, doors off	0.042	-0.074	-0.078	-0.092	-0.156	-----

The landing configuration is defined as slats extended, flaps deflected, landing gear down, and gear doors left on.

It can be seen in the preceding table that the stability changes encountered in going from the clean to the landing configuration were no greater than 3 percent  $\bar{c}_{50}$ . The model exhibited the least stability with slats and flaps retracted, landing gear extended, and gear doors left on.

A nose-down trim change was experienced in all intermediate configurations leading to and including the landing configuration regardless of whether slats and flaps were deflected first or last. The landing configuration had an increase in drag coefficient of about 0.116 over that of the clean model. Of this drag increase, about 0.079 was due to extending the slats and flaps. The lift-curve slope at  $C_L = 0.6$  remained essentially constant for all tail-on configurations listed in the preceding table and had a mean value of 0.085.

Longitudinal control.- The effect of elevator deflection on the longitudinal aerodynamic characteristics of the model is presented in figure 13. The elevator deflection required to trim the test model at a lift coefficient of 0.6 with a stabilizer setting of  $-\frac{3^\circ}{4}$  is listed in the preceding table as  $-4.5^\circ$  for the clean configuration and  $-10.2^\circ$  for the landing configuration. The data required to compute the trim elevator deflection of the clean configuration was obtained from reference 1. It was noted that adequate elevator effectiveness was available to trim the model over the lift coefficients obtainable in either configuration.

Characteristics in yaw.- Figure 14 shows that the directional stability of the clean model was essentially constant through the lift-coefficient range up to about  $C_{L_{max}}$ . The use of slats and flaps extended the stability to higher lift coefficients because of the increased maximum lift attainable. Directional instability was experienced after or very near the  $C_{L_{max}}$  of the model configuration in question. In general, good agreement was obtained with the data presented in reference 2 for the clean model and for the configuration utilizing slats and flaps. Extending the landing gear and leaving the gear doors open resulted in a decrease in directional stability from that of the configuration with slats and flaps extended although this decrease became less evident at high lift coefficients.

The effective dihedral of the clean model was increased by a fairly constant amount through the lift-coefficient range when slats and flaps were used. The extended landing gear and the open gear doors, however, tended to nullify this increase.

### The Effect of Dive Brakes

Characteristics in pitch.- Although the effect of the plug-type dive brakes on the stability characteristics of the clean model was satisfactory (see reference 3), figure 15 shows that an unstable stall is experienced if this type brake is used in conjunction with the landing configuration. Inasmuch as the unstable stall is evidenced in the tail-off pitching-moment curve, it can be assumed that the tail did not contribute significantly to this instability. In attempting to determine the cause of the unstable stall, tests were made with the rear landing-gear doors removed to simulate their being closed after the gear was down. The results presented in figure 16 indicate that the rear landing-gear doors did not contribute fundamentally to the instability at the stall. As a means of evaluating the effect of the rear doors without the dive brakes, tests were made of this configuration and the results are presented in figure 17.

With the tail and the rear landing-gear doors eliminated as the primary cause of the unstable stall of the model in the landing configuration with dive brakes extended, tuft studies of the flow on the wing were made. With dive brakes extended, an appreciable section of the wing inboard near the wing-fuselage juncture remained unstalled after flow separation of the rest of the wing was fairly complete. By inducing a premature separation in this region with a small spoiler located as shown in figure 6, a stable stall could be obtained. (See fig. 18.) In addition to the stable stall, some increase in longitudinal stability and drag was realized over the configuration without the spoiler.

If the plug-type dive-brake design were changed to that of the flap type having approximately the same frontal area, the flap-type dive brake would provide higher drag than that of the plug-type dive brake and spoiler. (See fig. 18.) A somewhat reduced stability resulting in slight instability above  $C_L = 0.9$  was obtained for the center-of-gravity and wing locations assumed. A stable stall, however, was experienced.

In view of the stable stall at  $20^\circ$  wing sweep, the effect of the flap-type dive brakes at  $60^\circ$  wing sweep was considered of interest. Figure 19 shows that a reduction in longitudinal stability was again obtained with very slight instability occurring near a lift coefficient of 0.7 when the flap-type dive brakes were used on the clean configuration with a  $60^\circ$  swept wing. At  $C_L = 0.8$ , stability was again evident up to and beyond the stall. The maximum lift coefficient as well as the lift-curve slope was reduced when the flap-type brakes were used. The drag coefficients at low lift coefficients were increased about 0.025 over those of the clean model.

Characteristics in yaw.- In view of the almost nonexistent effect of the plug-type dive brakes on the lateral-stability parameters of the clean configuration with  $20^\circ$  wing sweep (reference 3), tests of the

flap-type dive brakes on this configuration were not undertaken. When the flap-type dive brakes were used on the clean configuration with  $60^\circ$  sweep, an appreciable reduction in directional stability in the moderate lift-coefficient range was observed. (See fig. 20.) Directional instability occurred at a lift coefficient 0.17 below  $C_{L_{max}}$  compared to instability at a lift coefficient 0.23 below  $C_{L_{max}}$  for the clean model configuration. The instability of the model with dive brakes occurred, however, at a lower lift coefficient because of a reduction in  $C_{L_{max}}$ . Increases in the effective dihedral of varying magnitudes up to stall were observed when flap-type dive brakes were used, and, at the stall, values less negative than those of the clean configuration were encountered.

#### Effect of Gap at Wing Root

Characteristics in pitch.- The contemplated Bell X-5 airplane design includes a sliding fillet arrangement at the wing root that translates along the outside of the fuselage in conjunction with the wing. As a means of evaluating the effect of leakage through the fuselage at the wing root of the configuration with  $20^\circ$  wing sweep with slats and flaps extended, a few exploratory tests were made with a gap of roughly  $1/2$  inch around the wing root as shown in figure 6. This gap should produce much more extreme leakage than would be anticipated on the full-scale airplane and its effect on the test model would more than likely represent the outer boundary of the effect on the full-scale airplane. The over-all effect of the gap on the test model was what might be expected from the use of a wing of lower aspect ratio. The increase in longitudinal stability of the model with the gap open indicated an outward and rearward shift in the aerodynamic center due to unloading at the wing root (fig. 21). Although no tail-off tests were made, some reduction in downwash at the tail may have contributed to the longitudinal-stability increase. The lift-curve slope was reduced and the increase in drag became greater with increasing lift coefficient.

Characteristics in yaw.- The directional stability was again fairly constant with lift coefficient with some slight decrease noted over that of the configuration having the gap closed (fig. 22). The effective-dihedral variation with lift coefficient followed essentially the same trends as observed with the gap closed only with some slight decreases particularly in the high lift-coefficient range.

#### CONCLUSIONS

An investigation of the static stability and control characteristics at low speed of a  $\frac{1}{4}$ - scale model of a preliminary Bell X-5 airplane

design in the landing configuration has been conducted and the following conclusions have been drawn:

1. Changes in trim produced in going from the clean to the landing configuration would necessitate the use of a compensating elevator deflection of about  $-5.7^\circ$ . The longitudinal-stability changes encountered in going to the landing configuration were no greater than 3 percent of the mean aerodynamic chord at  $50^\circ$  sweep.

2. Adequate elevator effectiveness was available to trim to the maximum lift coefficients attainable in the landing configuration.

3. The use of plug-type fuselage dive brakes caused an unstable stall in the landing configuration but a stable stall could be obtained by addition of a small wing spoiler.

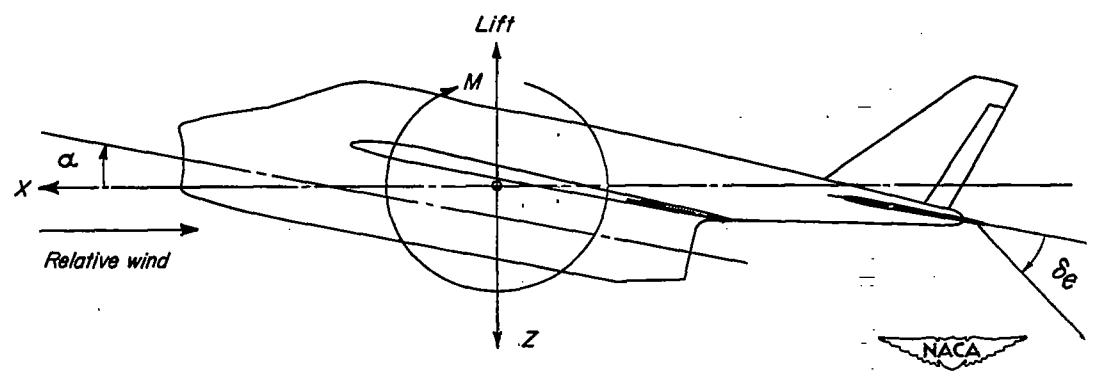
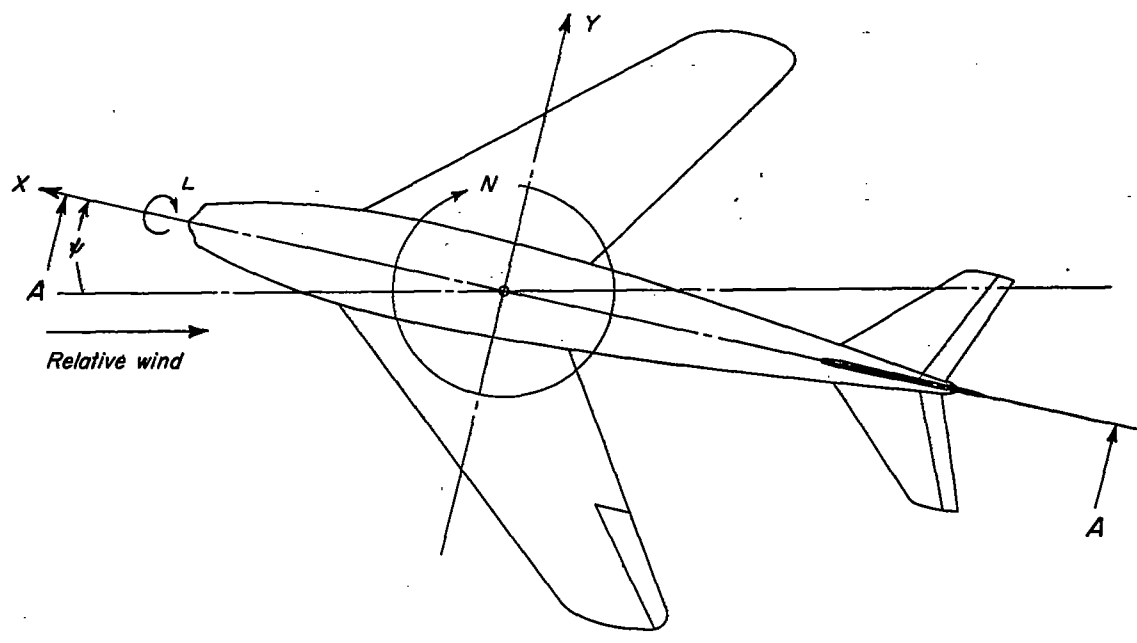
4. The use of flap-type fuselage dive brakes produced a stable stall, and also a general reduction in longitudinal stability over the lift-coefficient range with slight instability at the intermediate lift coefficients for both the  $20^\circ$  and  $60^\circ$  wing sweep angles.

5. Leakage through the fuselage at the wing root of the configuration with  $20^\circ$  sweep with slats and flaps extended increased the longitudinal stability and drag and, also, reduced the lift-curve slope.

Langley Aeronautical Laboratory  
National Advisory Committee for Aeronautics  
Langley Air Force Base, Va.

## REFERENCES

1. Kemp, William B., Jr., Becht, Robert E., and Few, Albert G., Jr.:  
Stability and Control Characteristics at Low Speed of a  $\frac{1}{4}$ -Scale  
Bell X-5 Airplane Model. Longitudinal Stability and Control.  
NACA RM L9K08, 1950.
2. Kemp, William B., Jr., and Becht, Robert E.: Stability and Control  
Characteristics at Low Speed of a  $\frac{1}{4}$ -Scale Bell X-5 Airplane Model.  
Lateral and Directional Stability and Control. NACA RM L50C17a,  
1950.
3. Becht, Robert E., and Few, Albert G., Jr.: Stability Characteristics  
at Low Speed of a  $\frac{1}{4}$ -Scale Bell X-5 Airplane Model with Various  
Modifications to the Basic Model Configuration. NACA RM L50F23,  
1950.
4. Gillis, Clarence L., Polhamus, Edward C., and Gray, Joseph L., Jr.:  
Charts for Determining Jet-Boundary Corrections for Complete Models  
in 7- by 10-Foot Closed Rectangular Wind Tunnels. NACA ARR L5G31,  
1945.
5. Herriot, John G.: Blockage Corrections for Three-Dimensional-Flow  
Closed-Throat Wind Tunnels, with Consideration of the Effect of  
Compressibility. NACA RM A7B28, 1947.

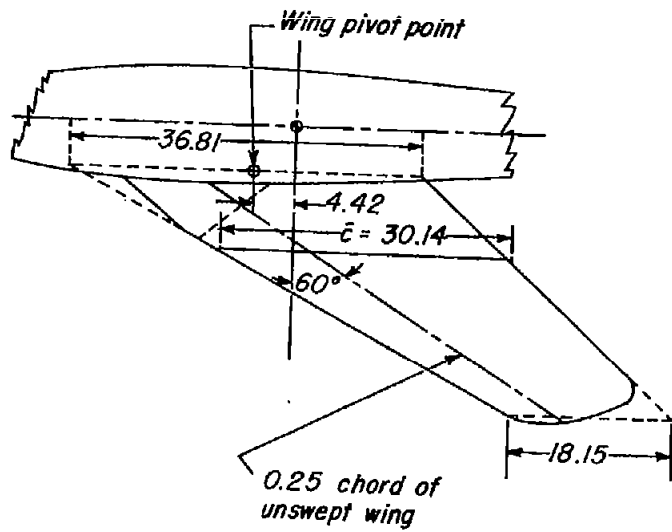


View A-A

Figure 1.- System of axes and control-surface deflections. Positive values of forces, moments, and angles are indicated by arrows.



CONFIDENTIAL



0 10 20  
Scale, inches

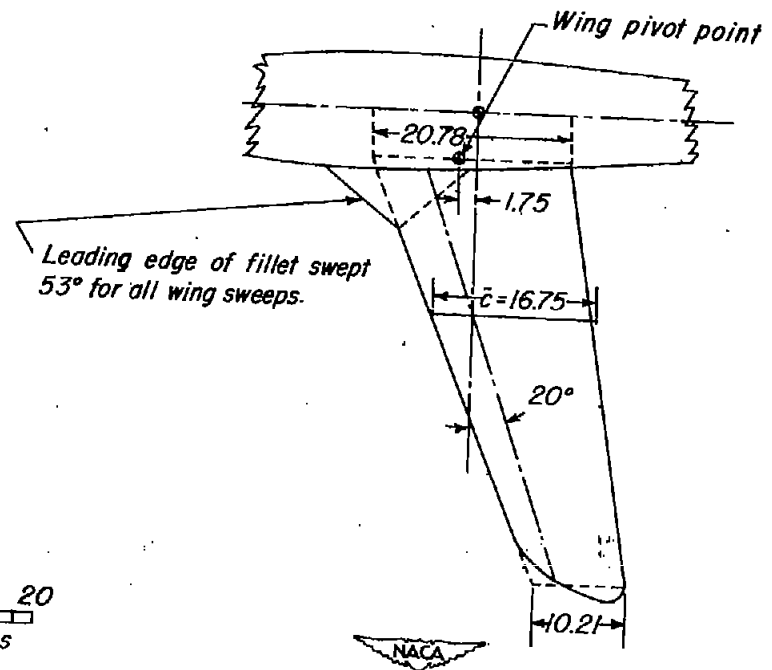


Figure 2.- Concluded.

CONFIDENTIAL

NACA RM L50J27

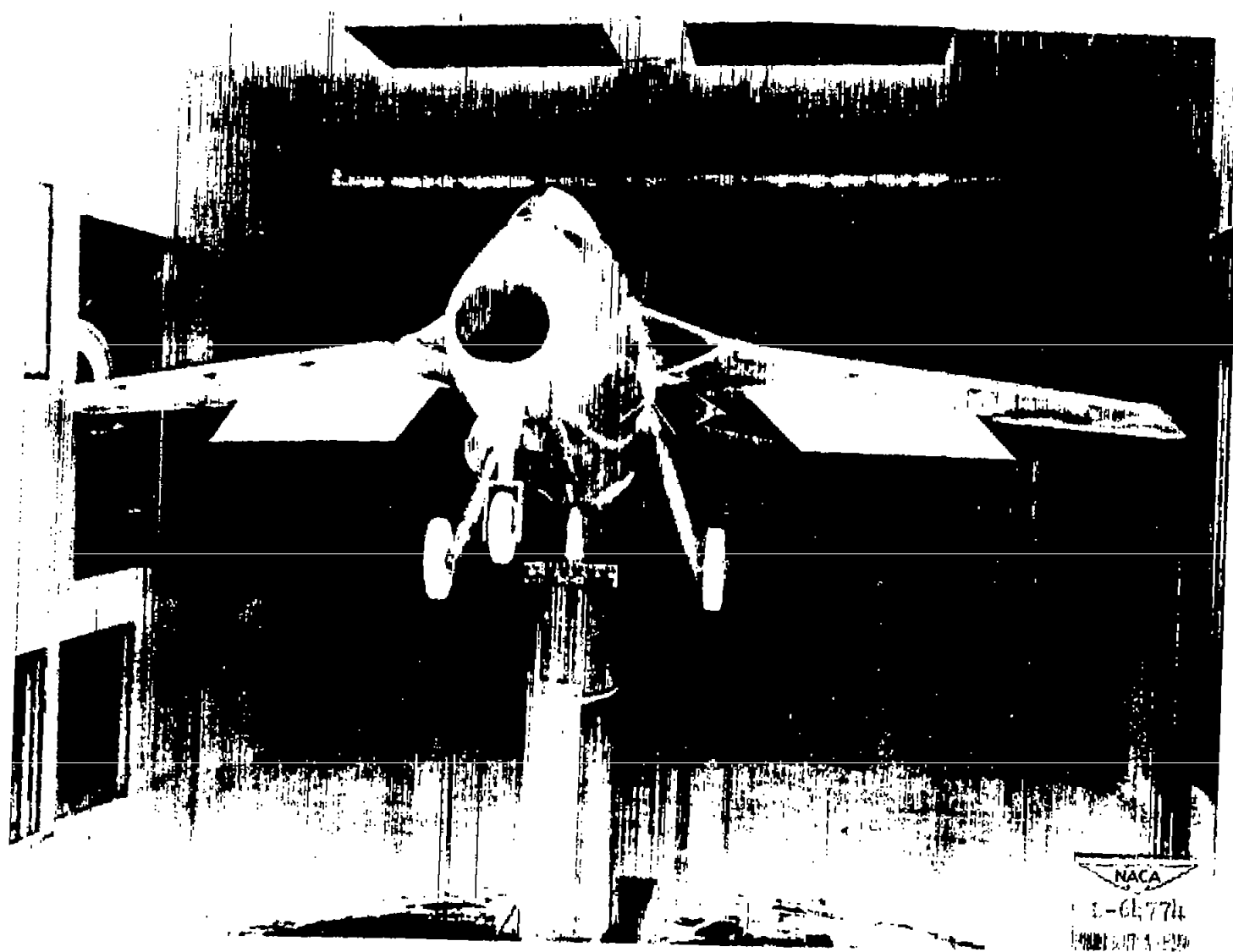
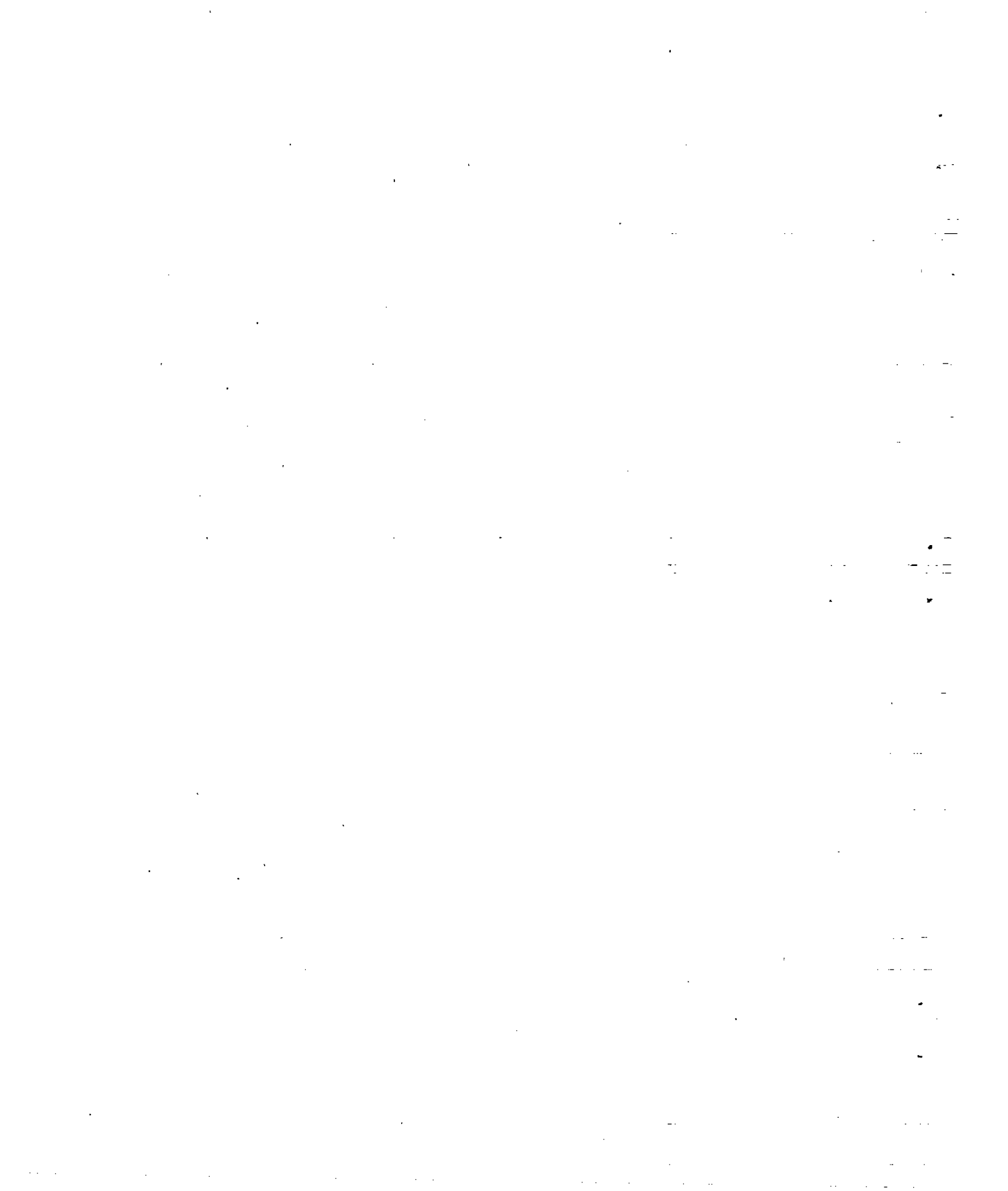


Figure 3.- Views of test model mounted in tunnel.



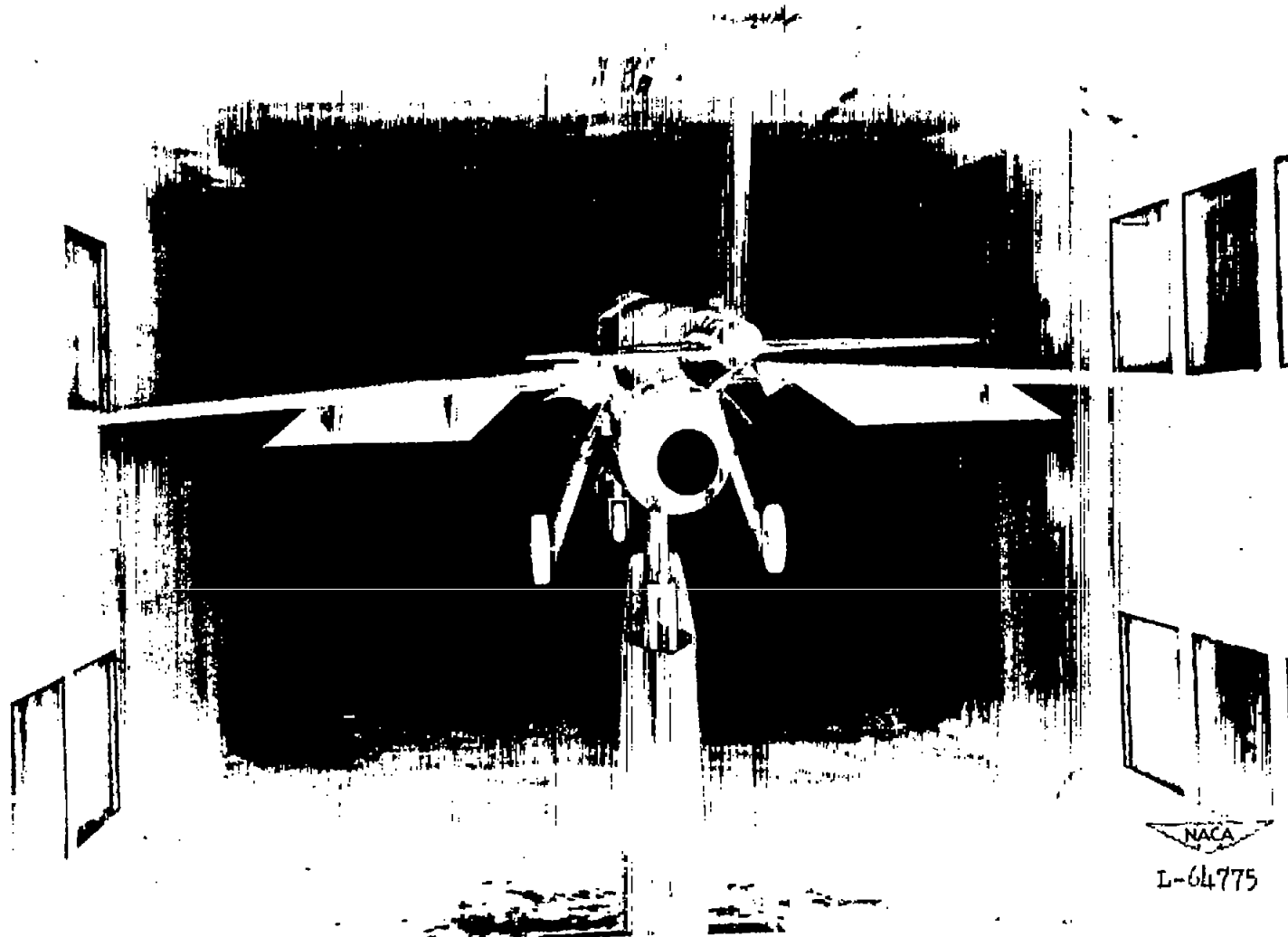
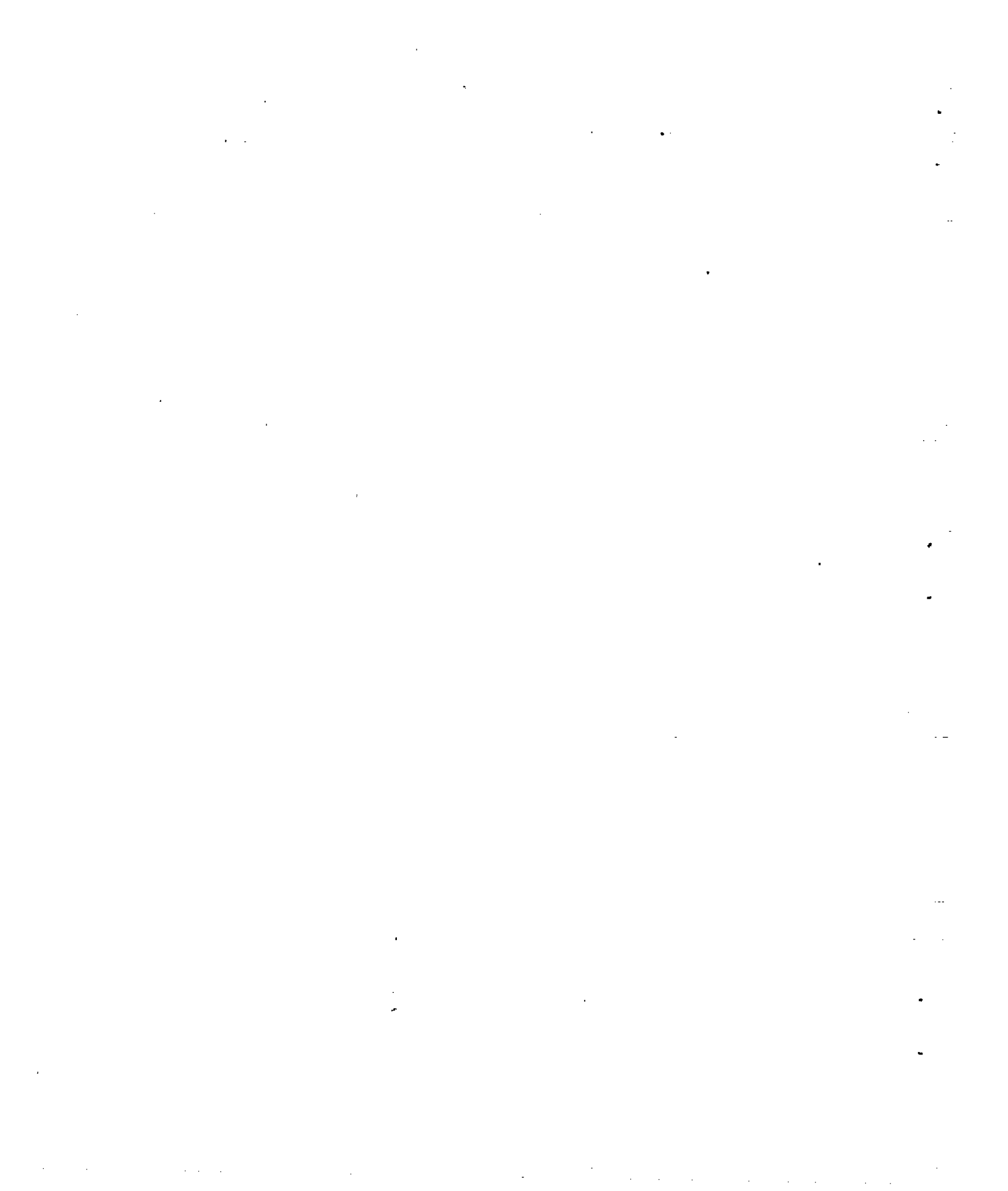
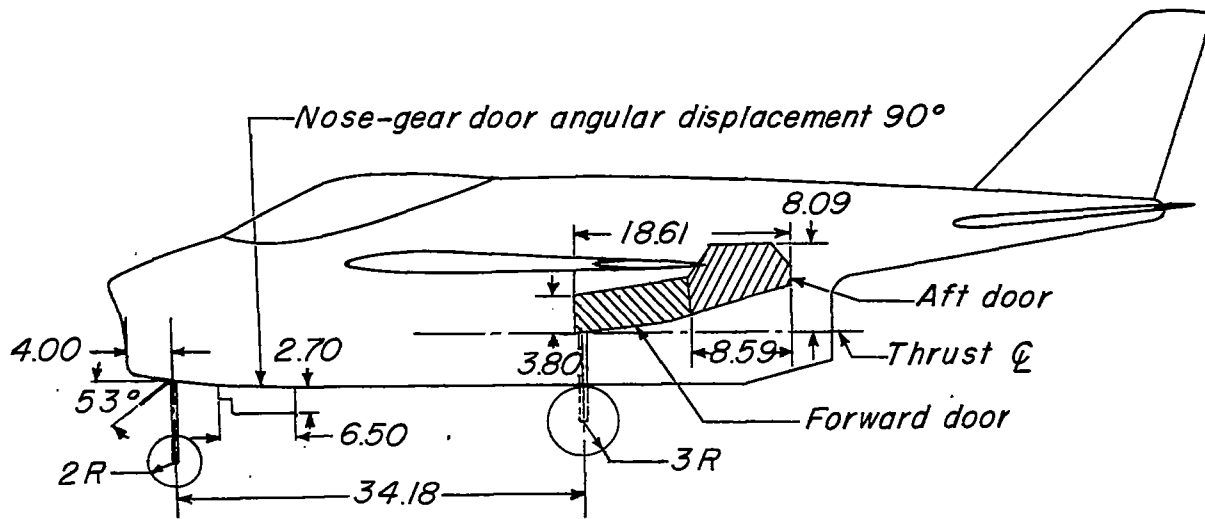


Figure 3.- Concluded.





*Elevation projection of landing gear doors.  
Doors flush in closed position; angular  
displacements for full open positions are:  
forward door  $39^\circ$   
aft door  $55^\circ$*

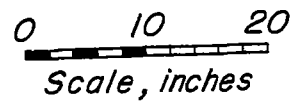
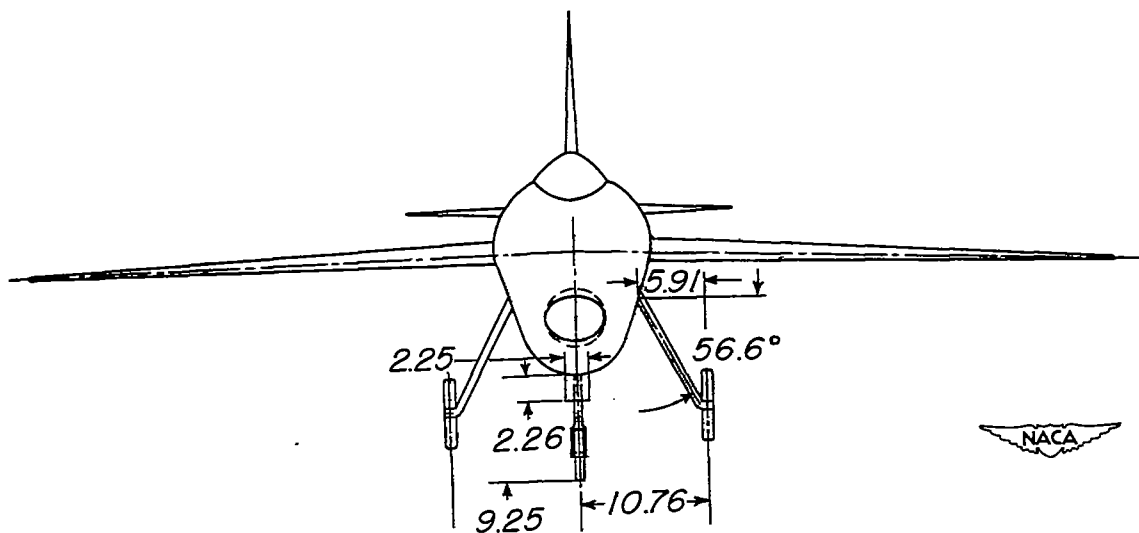
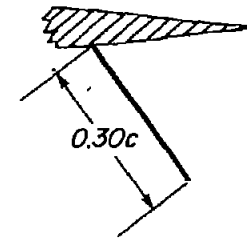
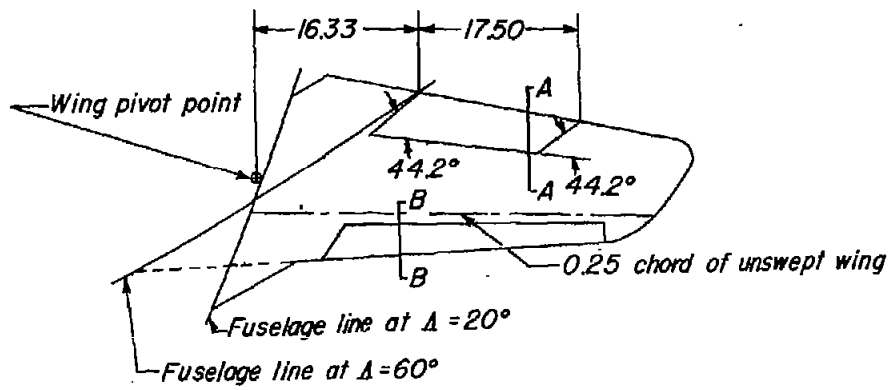
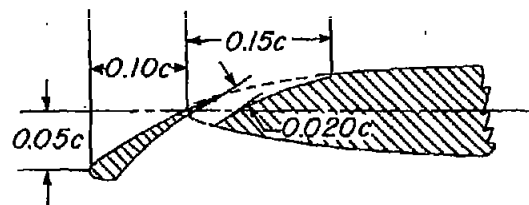


Figure 4.- Details of the landing gear and doors.



Section A-A

Split flap



Section B-B

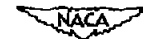
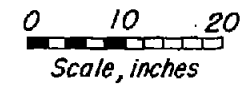


Figure 5.- Details of flap and slat.

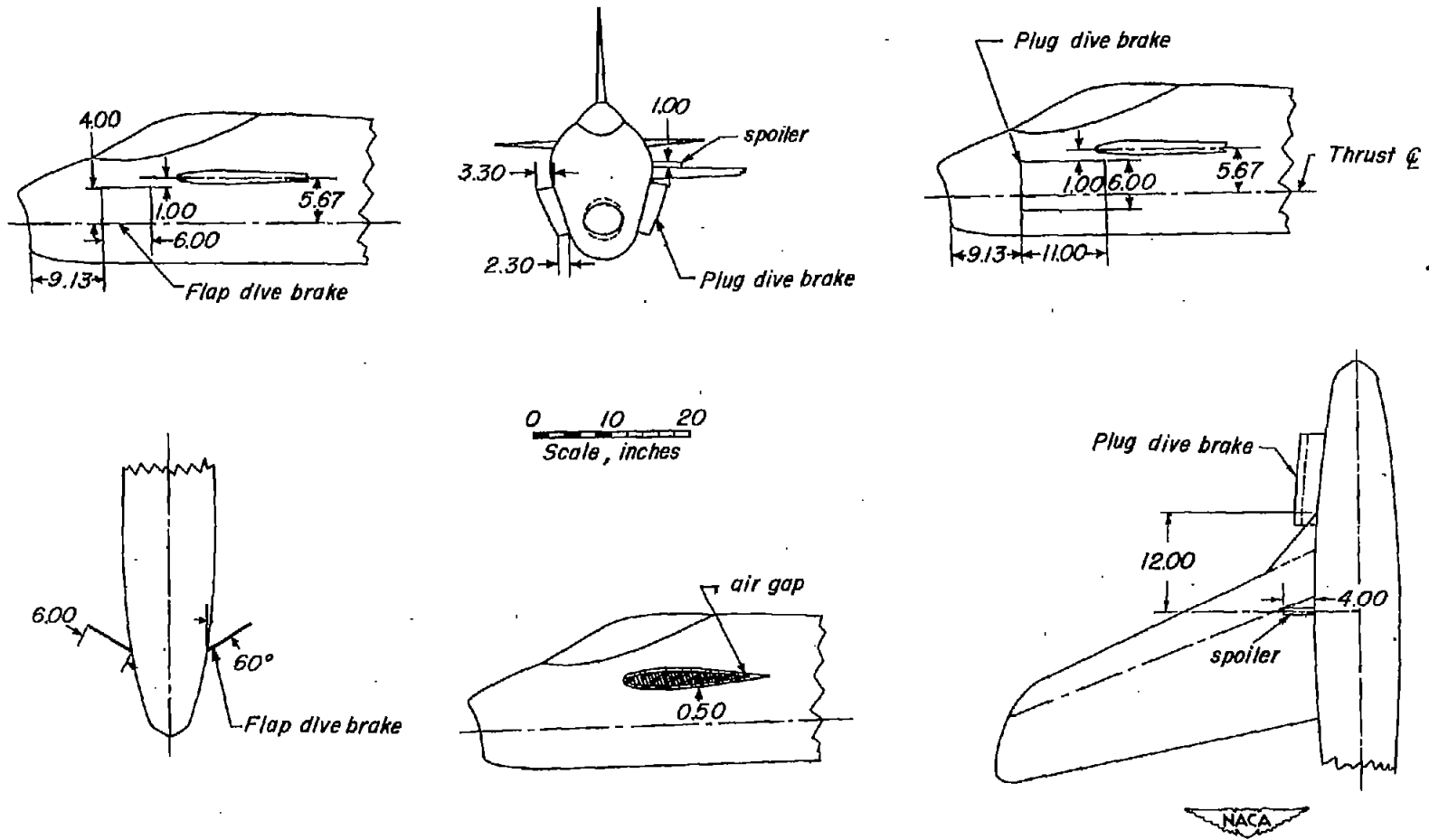


Figure 6.- Details of dive brakes, air gap, and spoiler.

CONFIDENTIAL

CONFIDENTIAL

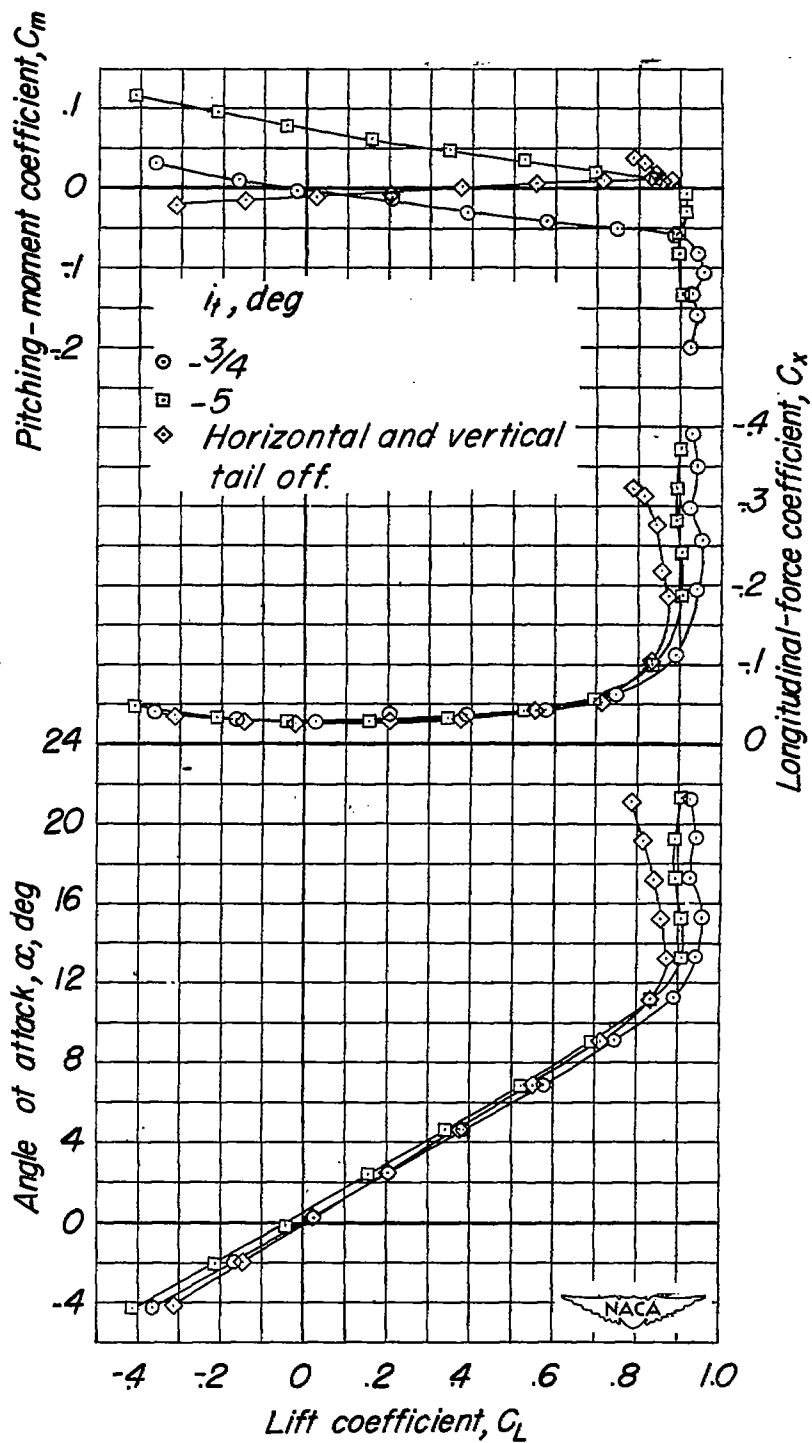


Figure 7.- The effect of tail incidence on the aerodynamic characteristics of the test model.  $\Lambda = 20^\circ$ ; slats retracted;  $\delta_f = 0^\circ$ ; landing gear and gear doors off.

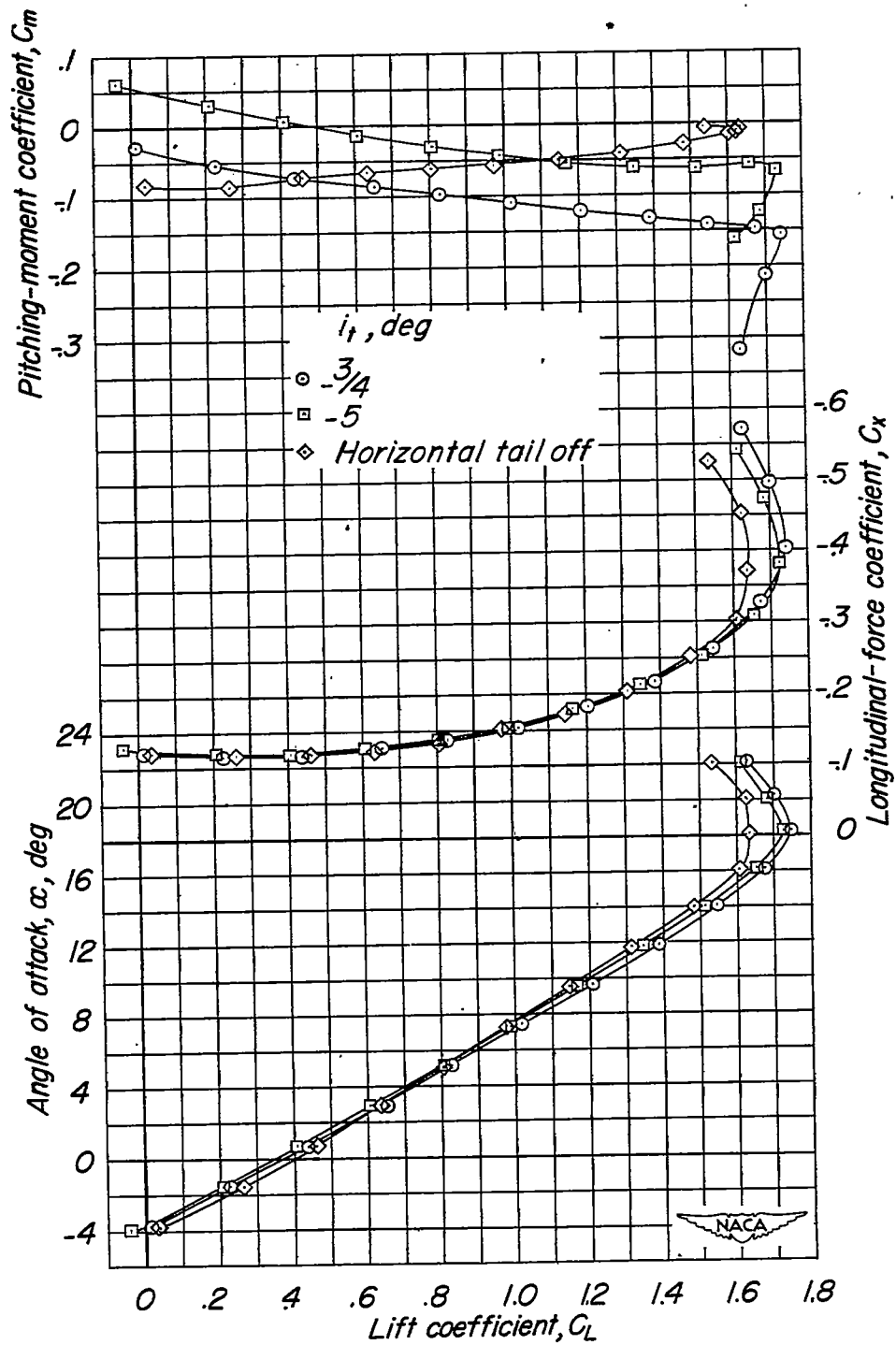


Figure 8.- The effect of tail incidence on the aerodynamic characteristics of the test model.  $\Lambda = 20^\circ$ ; slats extended;  $\delta_f = 50^\circ$ ; landing gear and gear doors off.

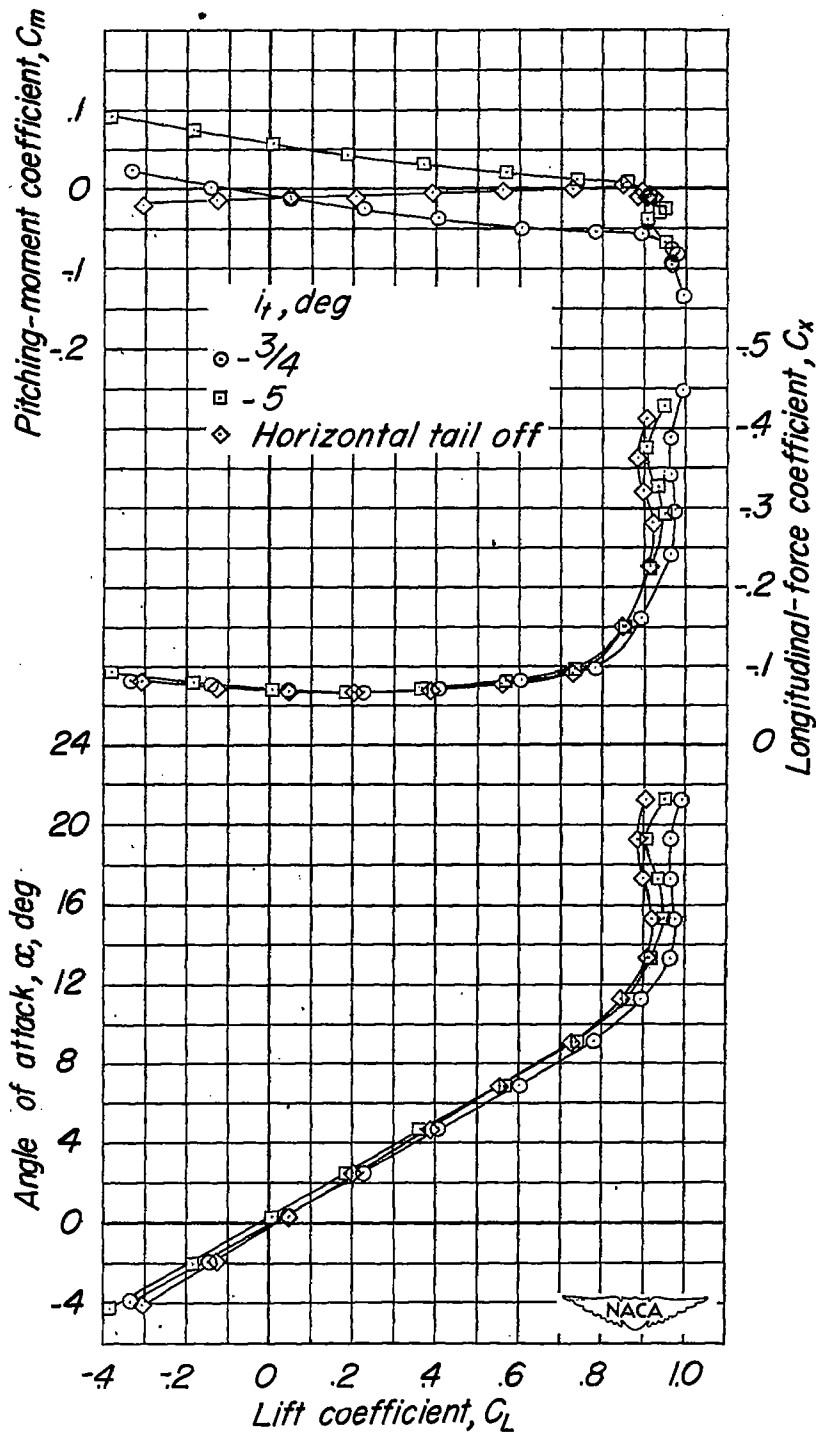


Figure 9.- The effect of tail incidence on the aerodynamic characteristics of the test model.  $\Lambda = 20^\circ$ ; slats retracted;  $\delta_F = 0^\circ$ ; landing gear extended and gear doors open.

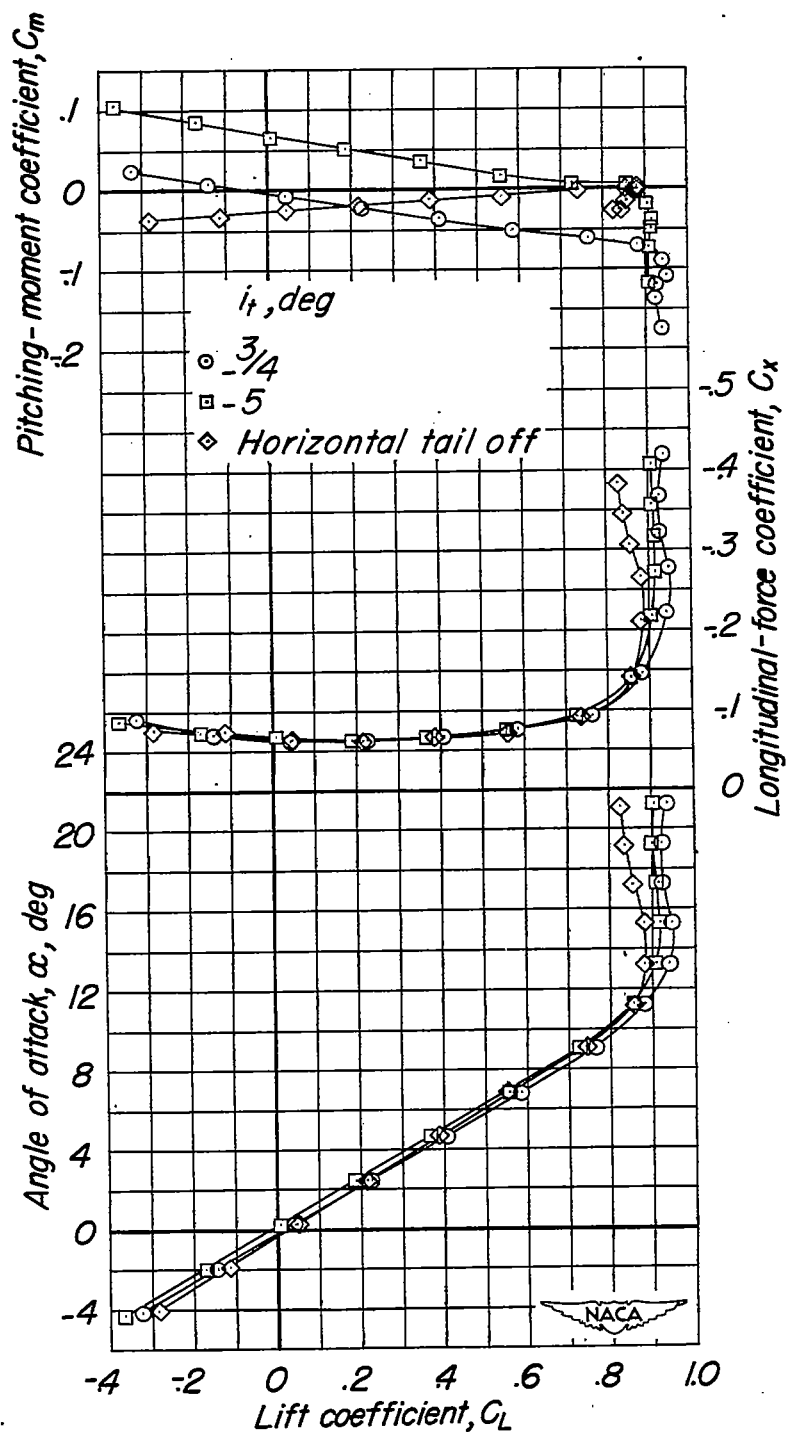


Figure 10.- The effect of tail incidence on the aerodynamic characteristics of the test model.  $\Lambda = 20^\circ$ ; slats retracted;  $\delta_f = 0^\circ$ ; landing gear extended and gear doors off.

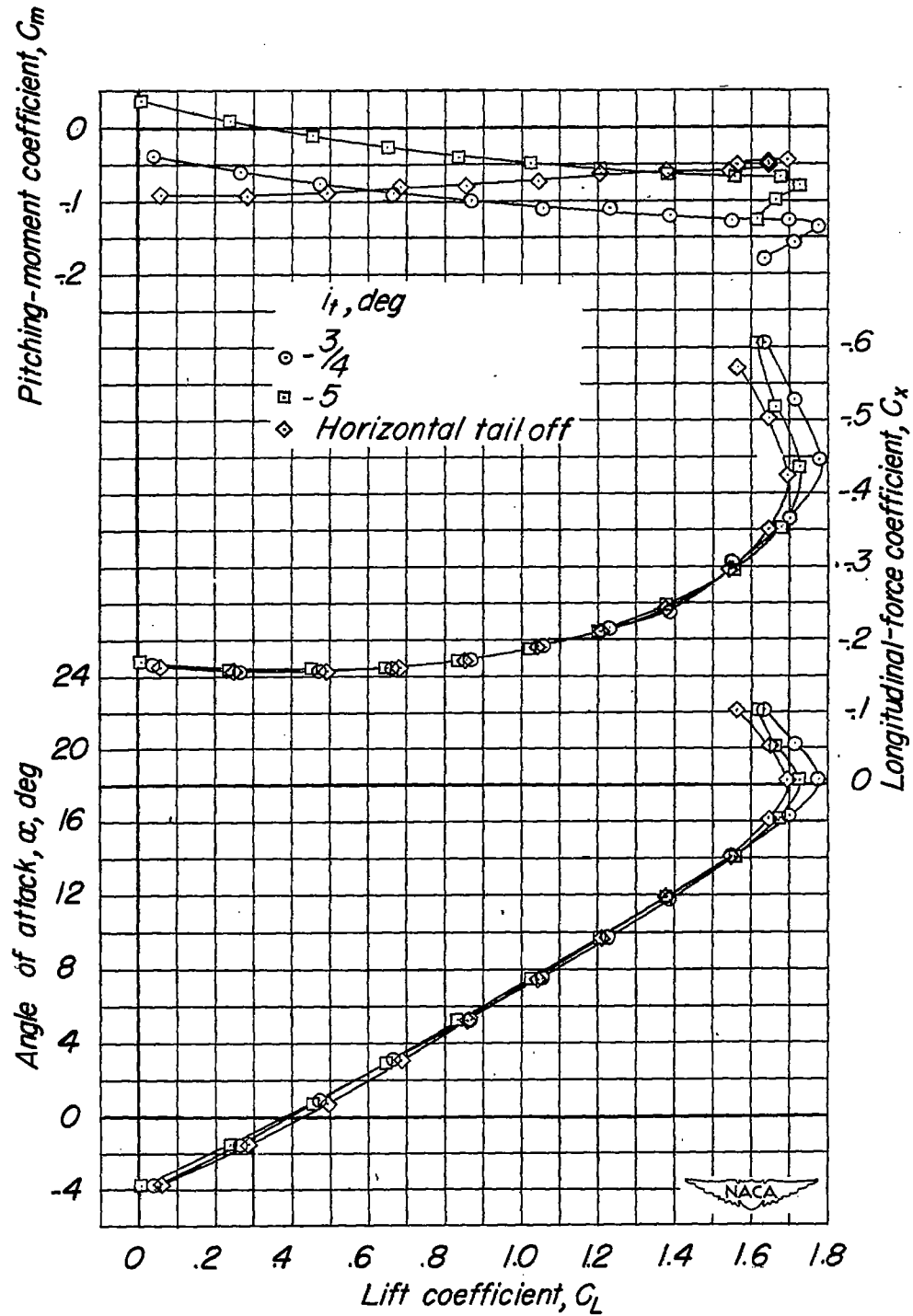


Figure 11.- The effect of tail incidence on the aerodynamic characteristics of the test model.  $\Lambda = 20^\circ$ ; slats extended;  $\delta_F = 50^\circ$ ; landing gear extended and gear doors open.

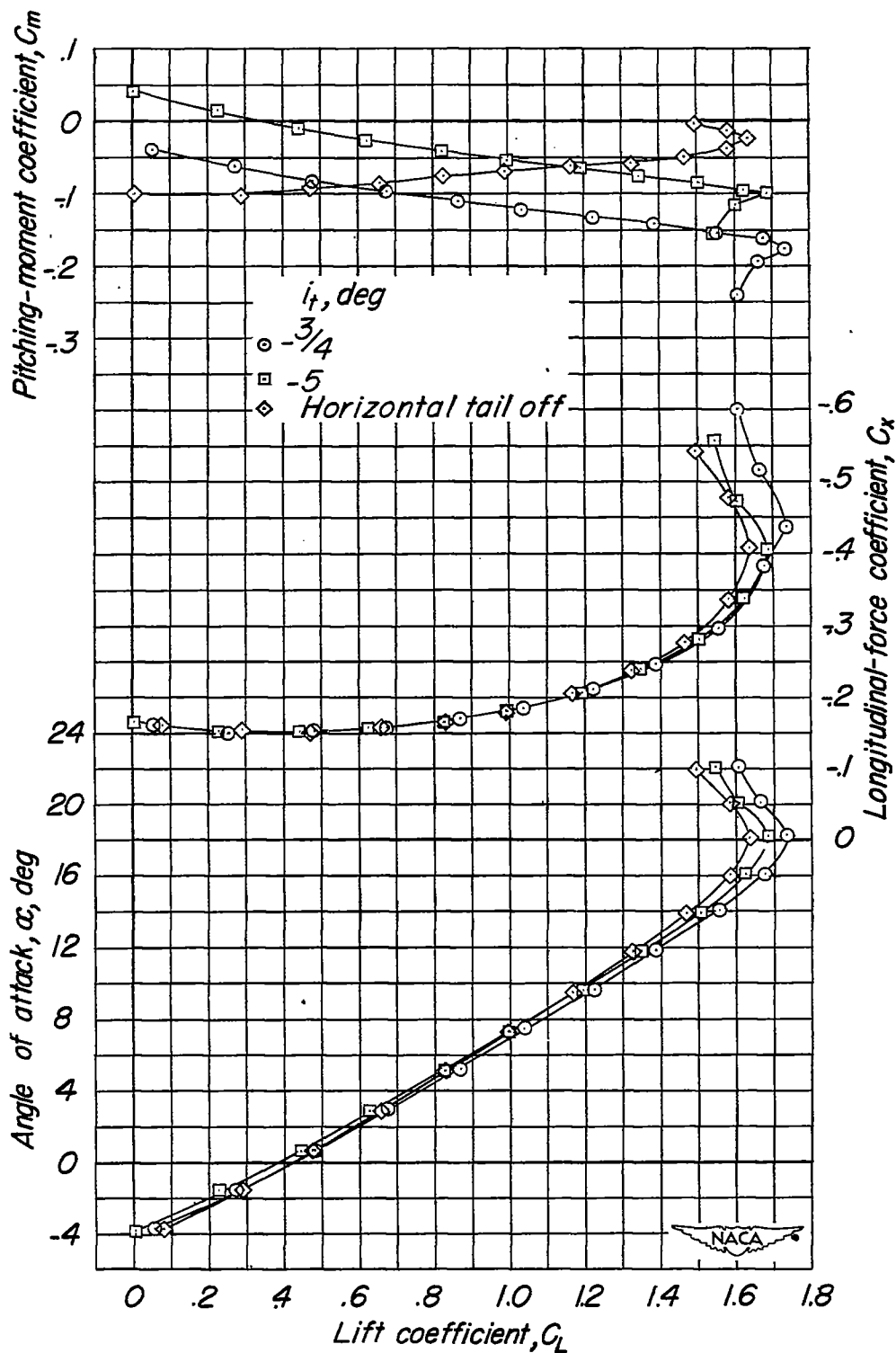


Figure 12.- The effect of tail incidence on the aerodynamic characteristics of the test model,  $\Lambda = 20^\circ$ ; slats extended;  $\delta_f = 50^\circ$ ; landing gear extended and gear doors off.

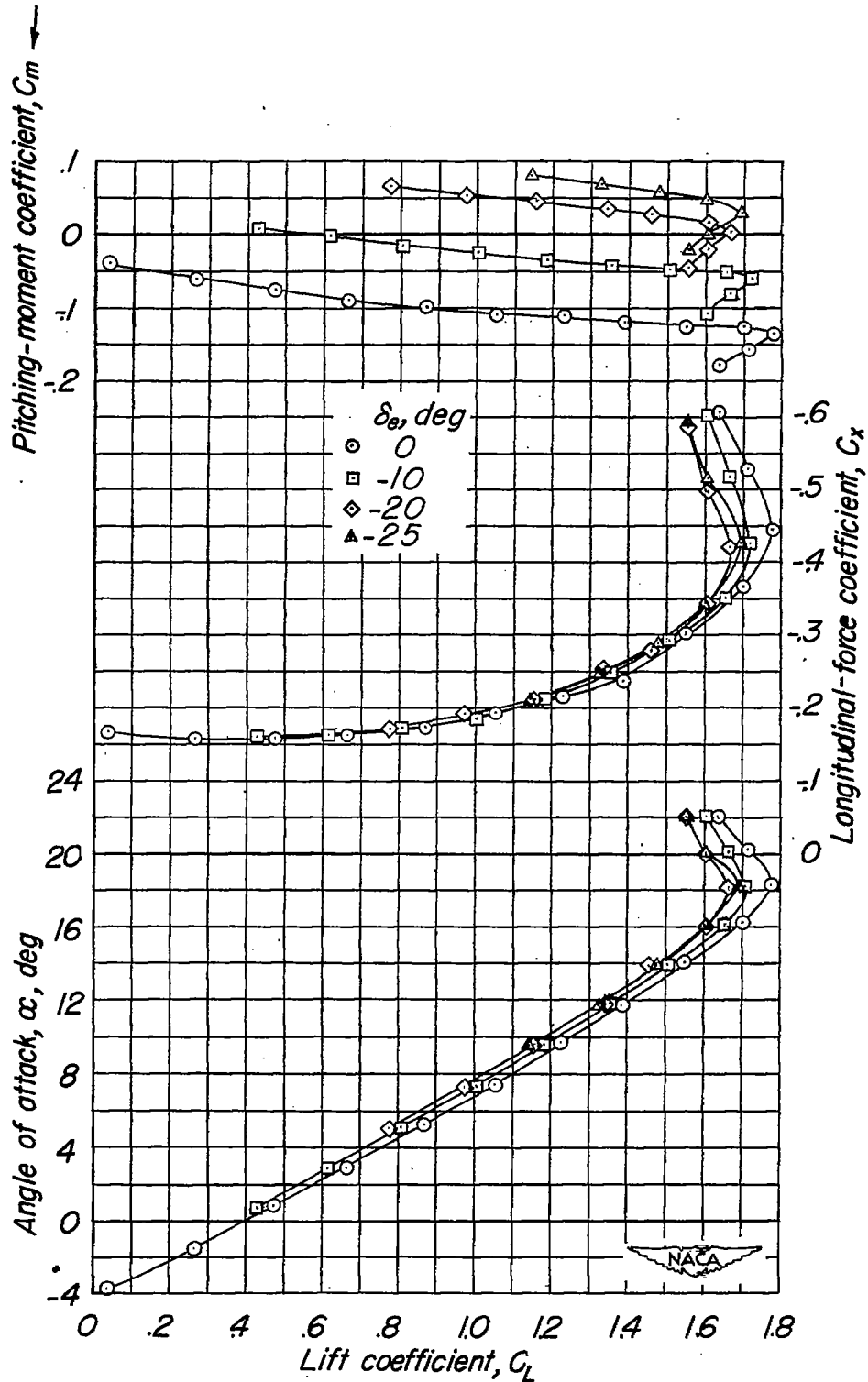


Figure 13.- The effect of elevator deflection on the aerodynamic characteristics of the test model.  $\Lambda = 20^\circ$ ; slats extended;  $\delta_f = 50^\circ$ ; landing gear extended and gear doors open.

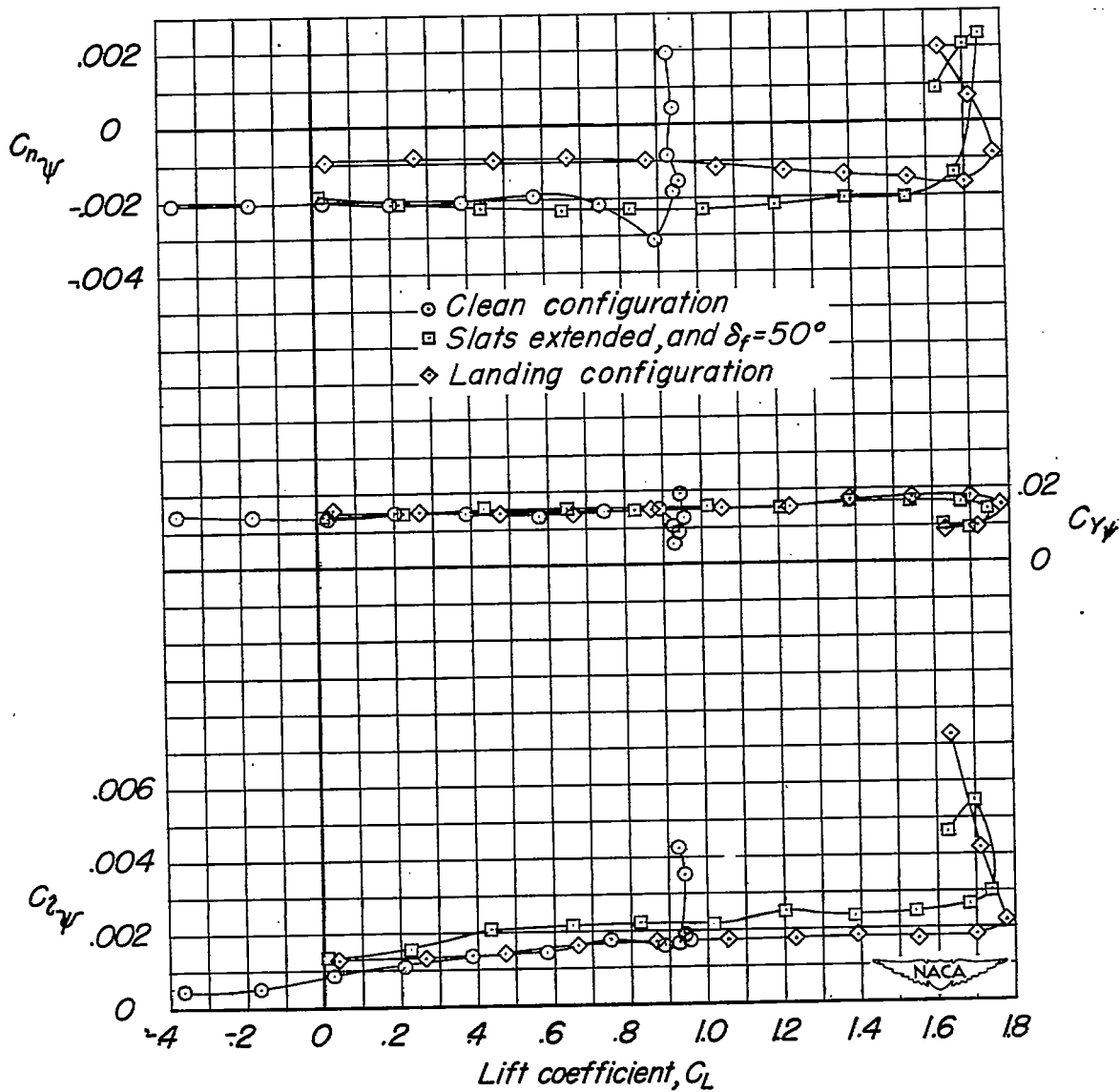


Figure 14.- The effect of slats and flaps, and the landing configuration on the lateral-stability parameters of the clean model.  $\Lambda = 20^\circ$ .

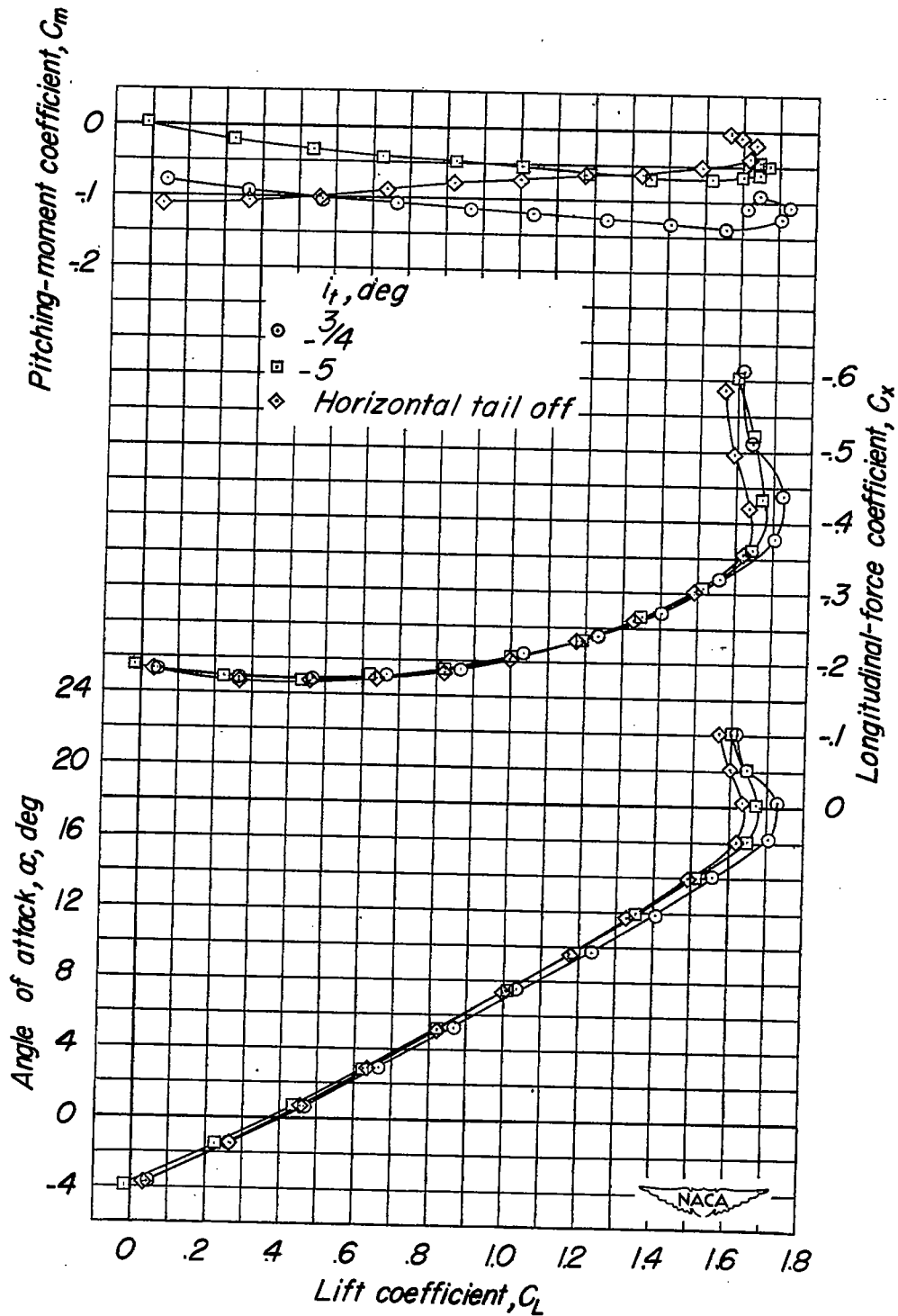


Figure 15.- The effect of tail incidence on the aerodynamic characteristics of the test model.  $\Lambda = 20^\circ$ ; slats extended;  $\delta_f = 50^\circ$ ; landing gear extended; gear doors open and plug-type dive brakes extended.

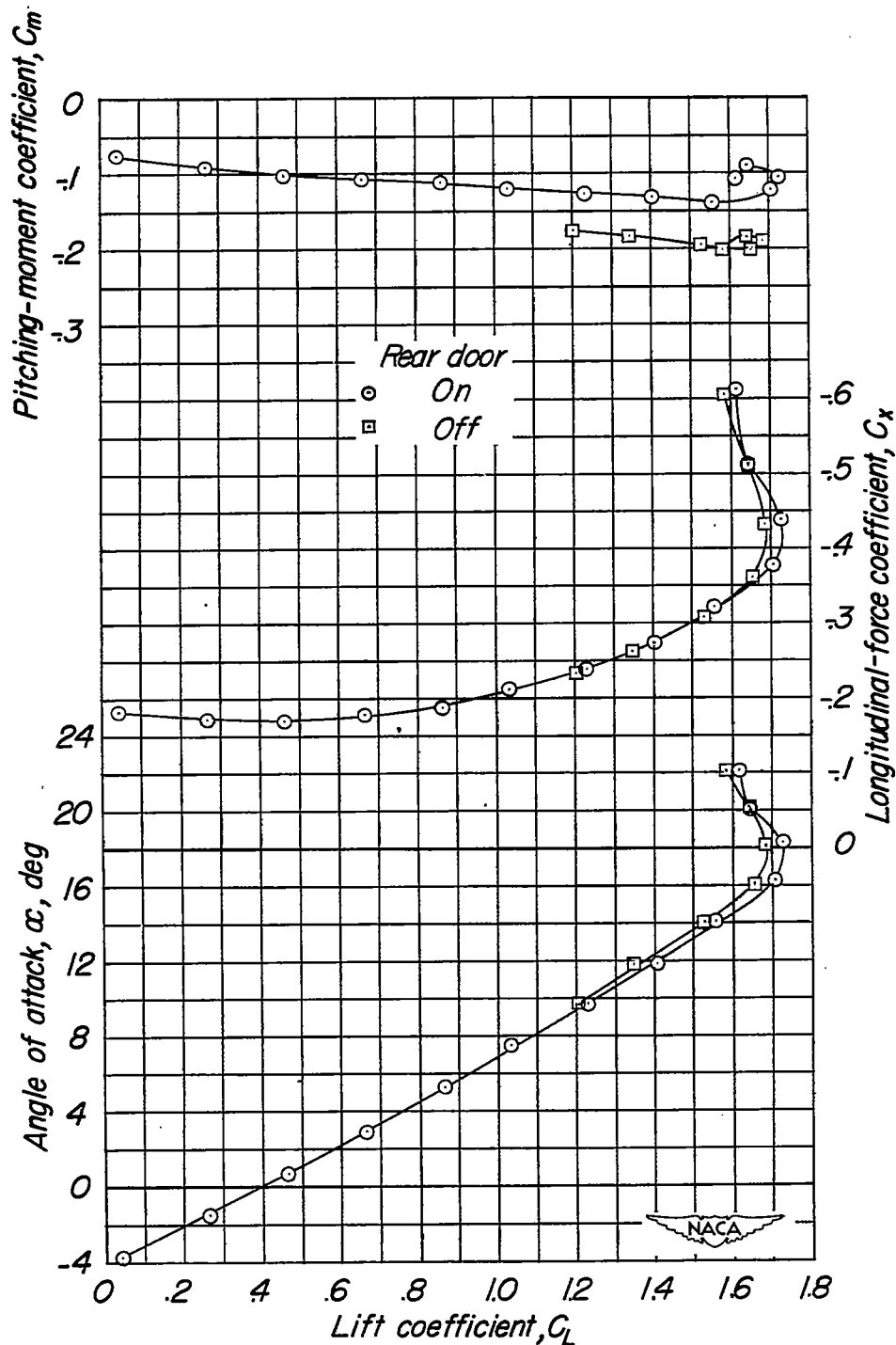


Figure 16.- The effect of the rear landing-gear doors on the aerodynamic characteristics of the test model.  $\Lambda = 20^\circ$ ;  $i_t = -\frac{3^\circ}{4}$ ; slats extended;  $\delta_f = 50^\circ$ ; landing gear extended; nose wheel doors and front main gear doors open; and plug-type dive brake extended.

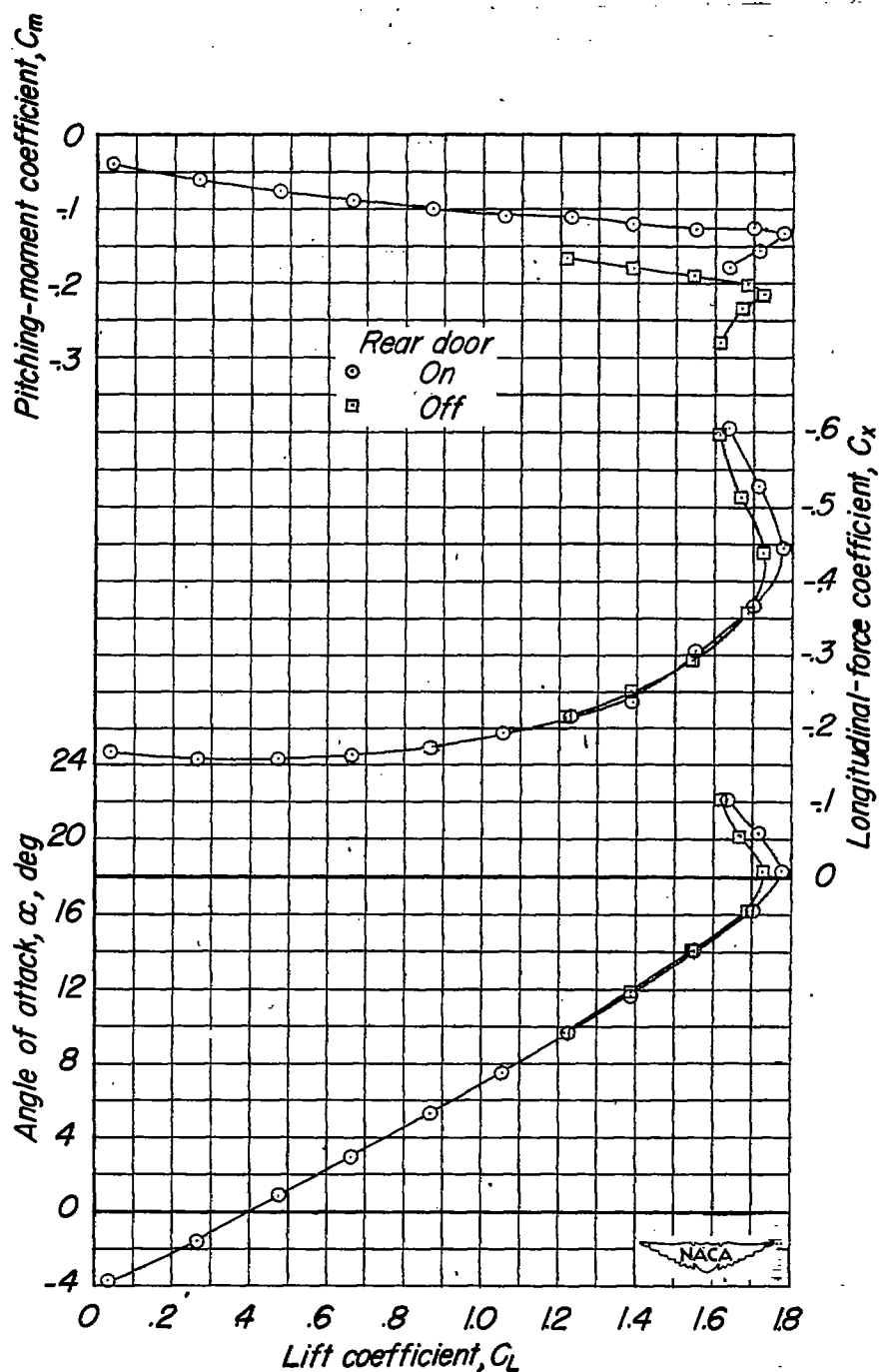


Figure 17.- The effect of the rear landing-gear doors on the aerodynamic characteristics of the test model.  $\Lambda = 20^\circ$ ;  $i_t = -\frac{3^\circ}{4}$ ; slats extended;  $\delta_f = 50^\circ$ ; landing gear extended; nose wheel doors and front main gear doors open; plug-type dive brakes off.

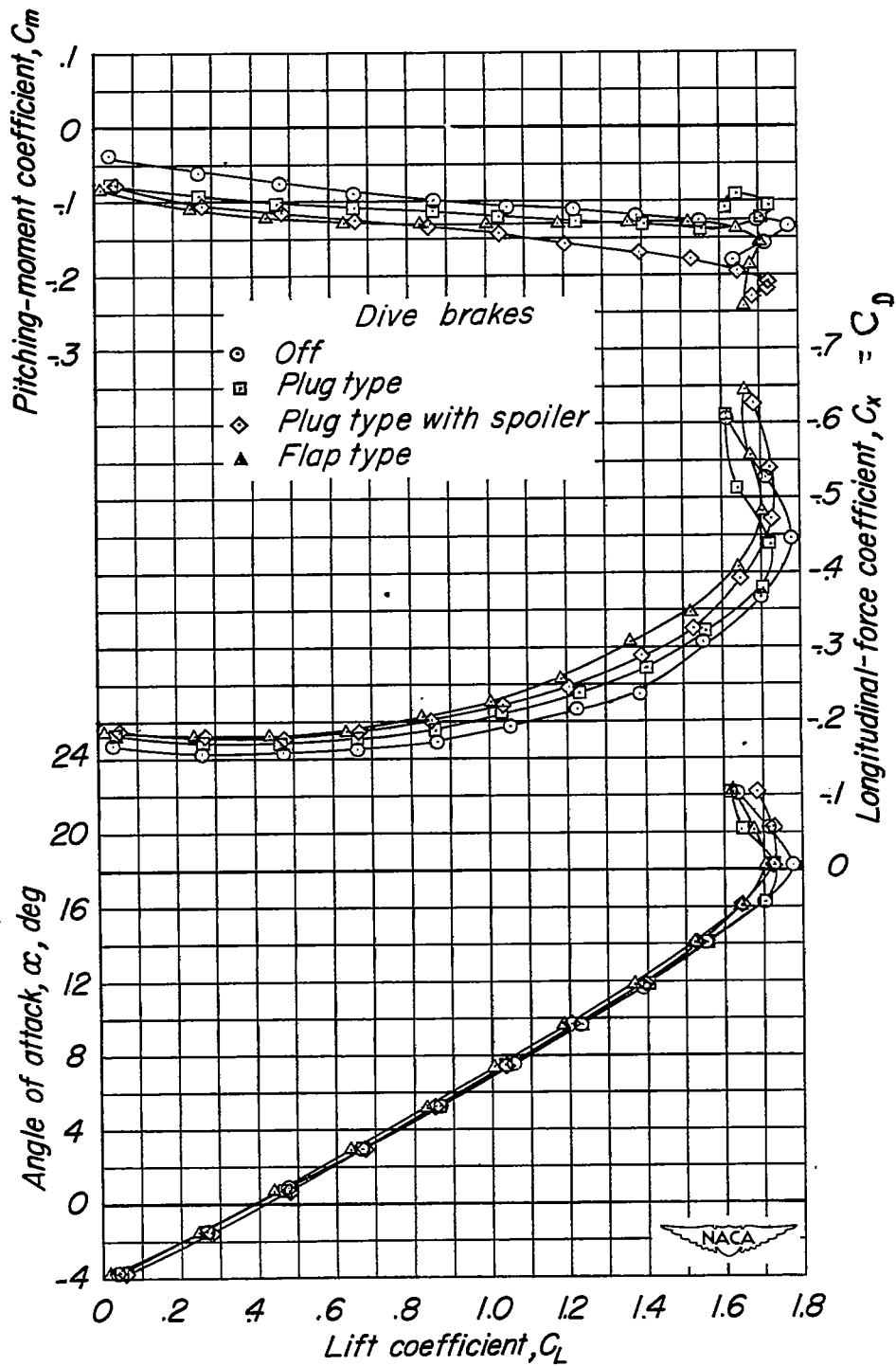


Figure 18.- The effect of dive brakes on the aerodynamic characteristics of the test model.  $\Lambda = 20^\circ$ ;  $i_t = -\frac{3^\circ}{4}$ ; slats extended;  $\delta_f = 50^\circ$ ; landing gear extended; and gear doors open.

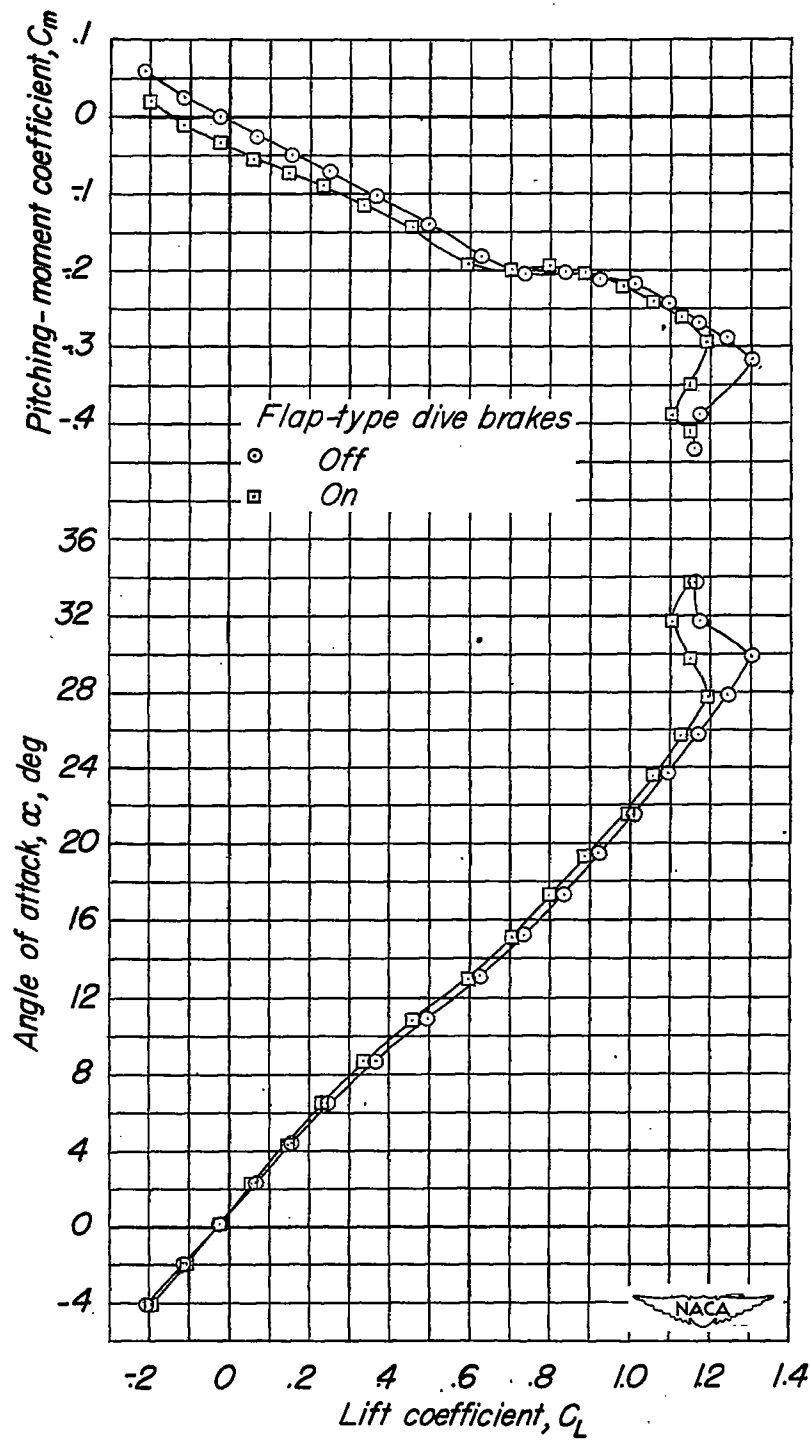


Figure 19.- The effect of the flap-type dive brakes on the aerodynamic characteristics of the clean model.  $\Lambda = 60^\circ$ ;  $i_t = -\frac{3^\circ}{4}$ .

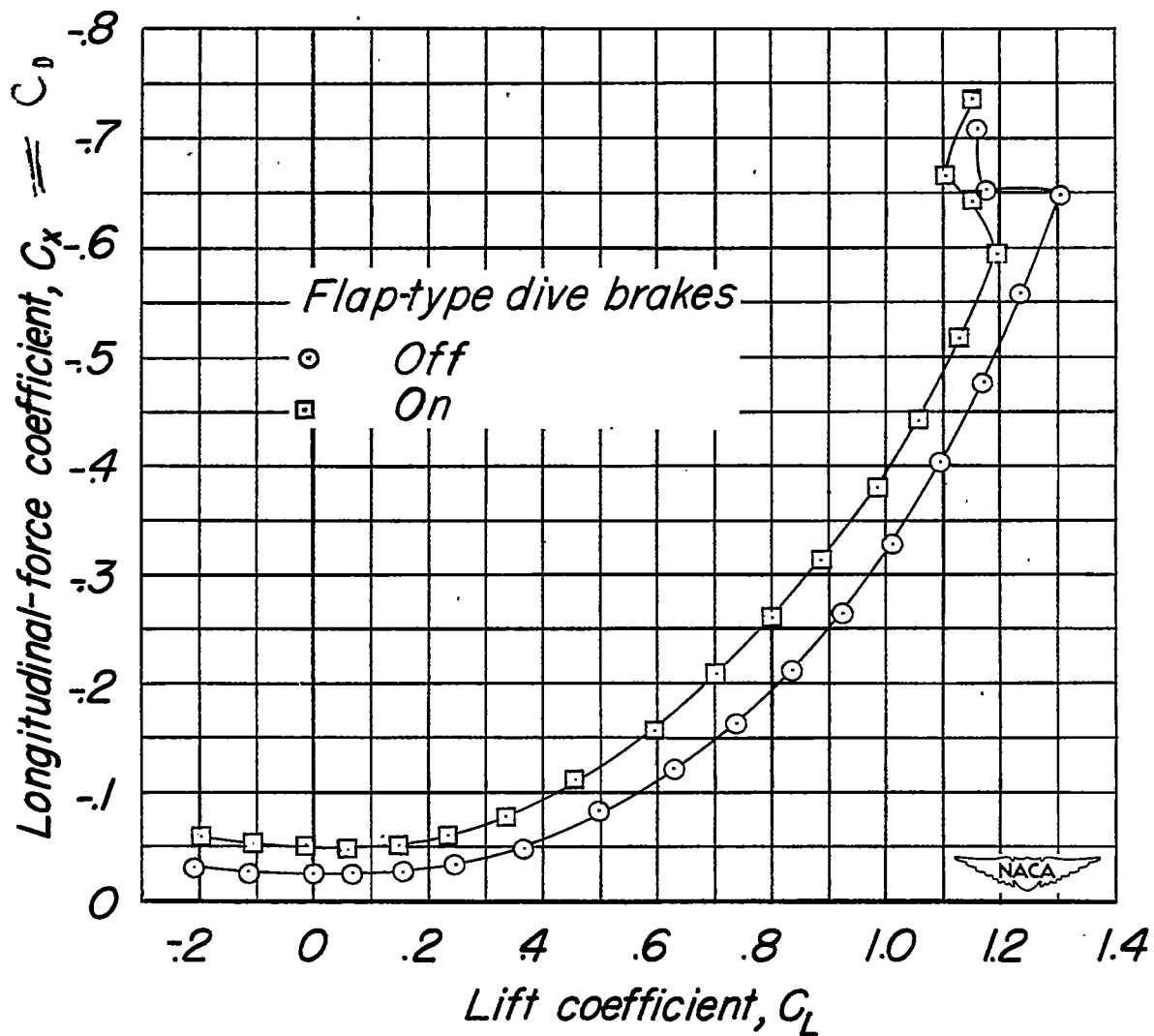


Figure 19.- Concluded.

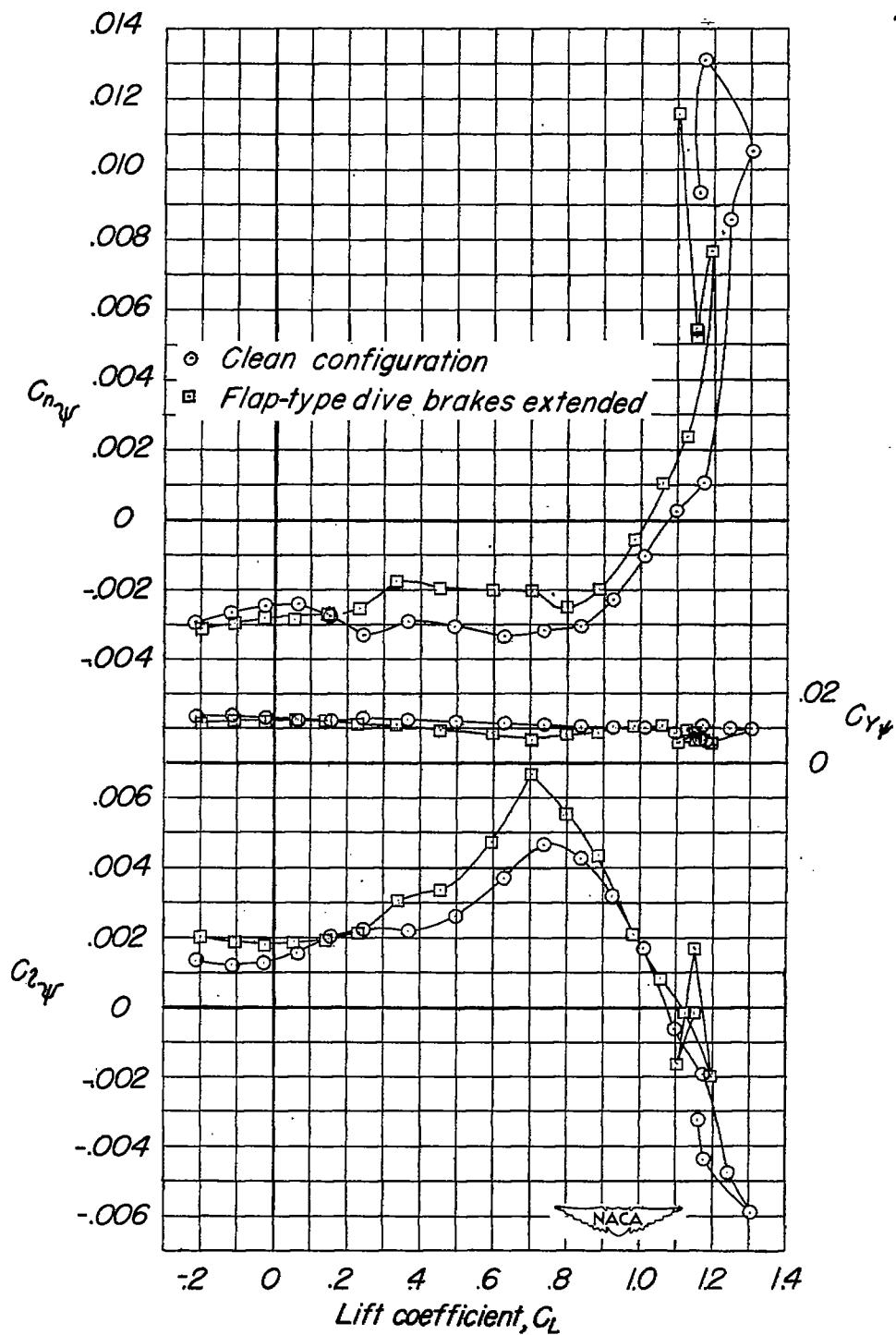


Figure 20.- The effect of the flap-type dive brakes on the lateral stability characteristics of the clean model.  $\Lambda = 60^\circ$ ;  $i_t = -\frac{3^\circ}{4}$ .

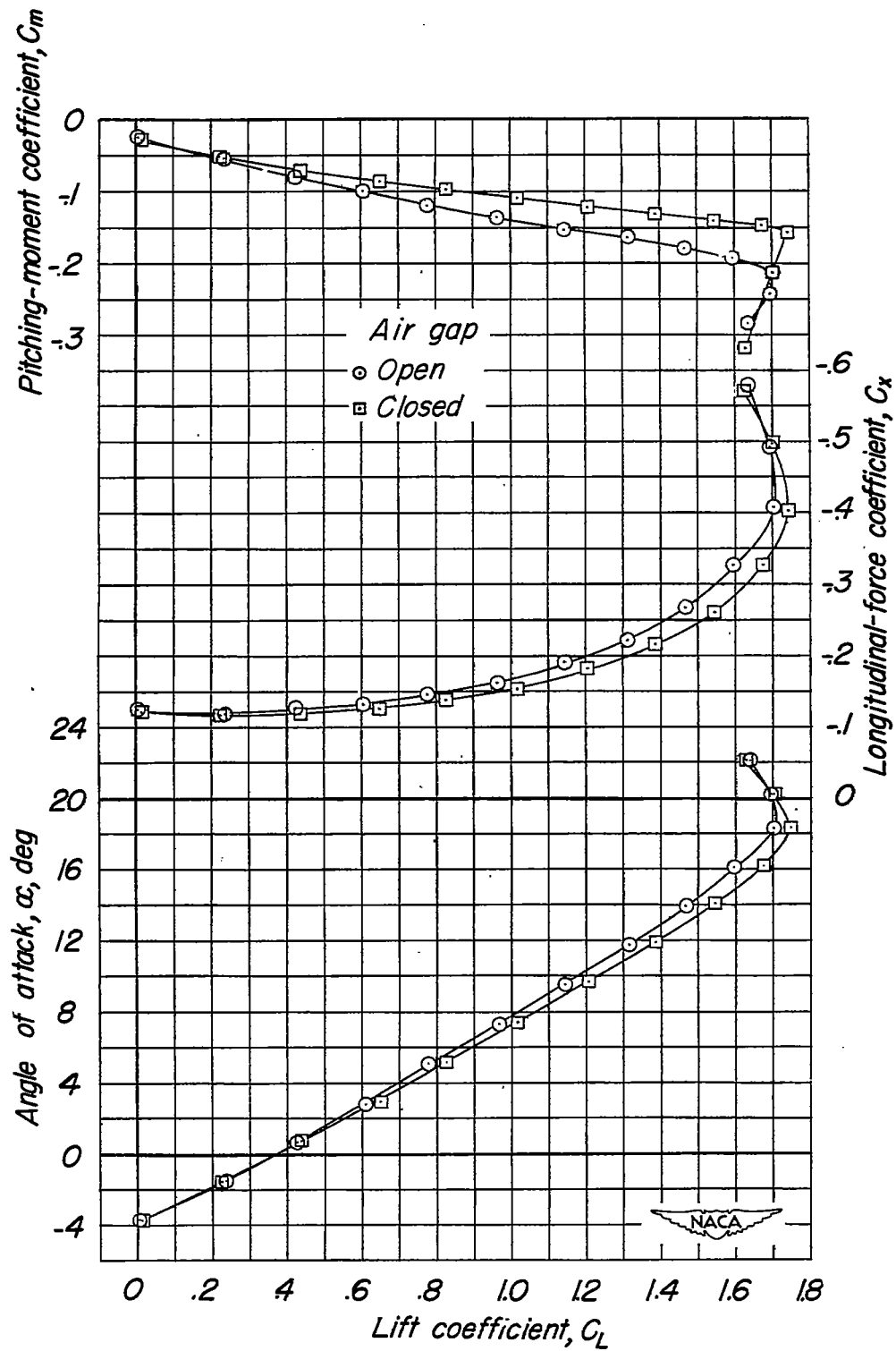


Figure 21.- The effect of the air gap in the fuselage on the aerodynamic characteristics of the test model.  $\Lambda = 20^\circ$ ; slats extended;  $\delta_f = 50^\circ$ .

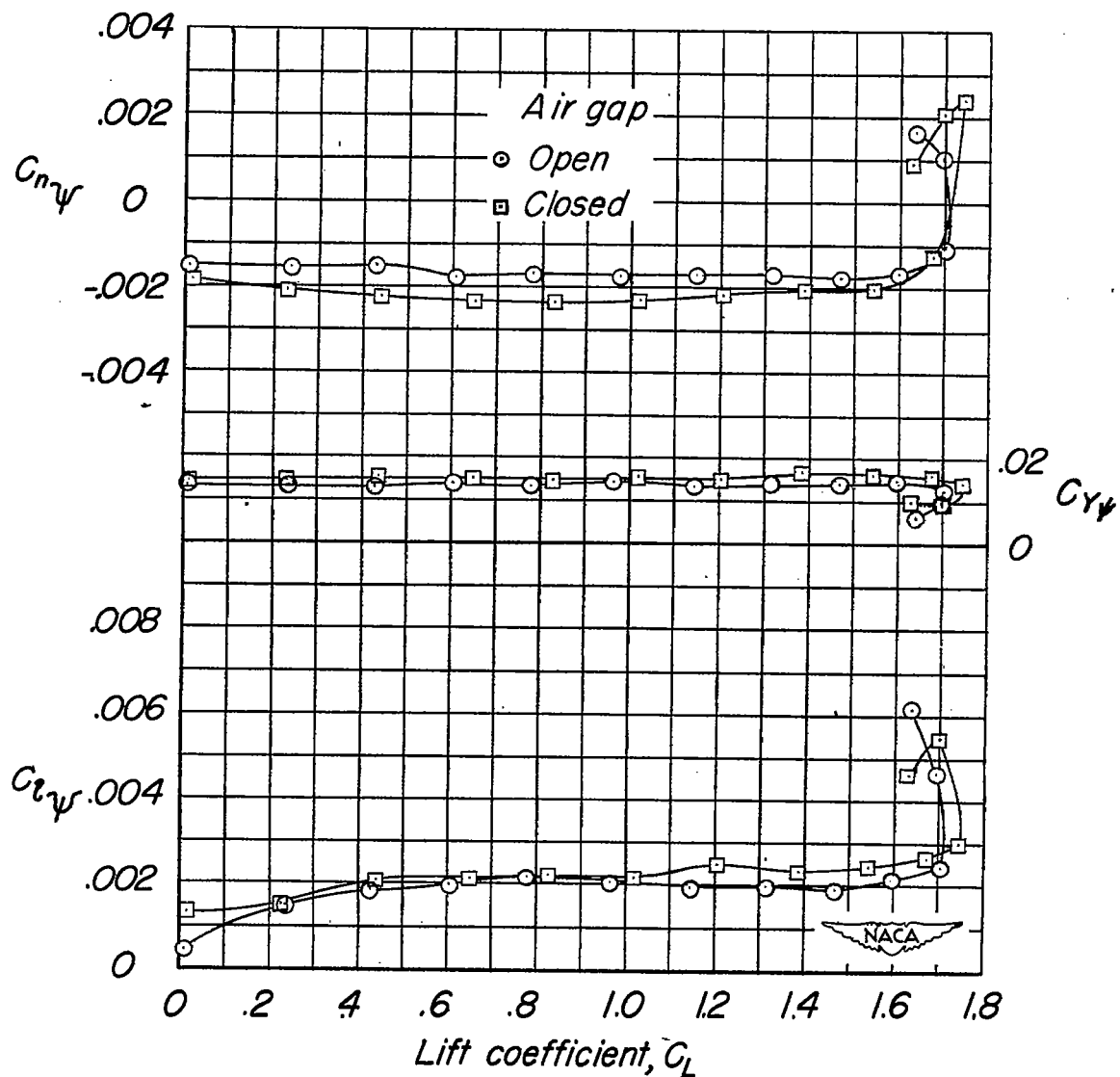


Figure 22.- The effect of the air gap in the fuselage on the lateral-stability parameters of the test model.  $\Lambda = 20^\circ$ ;  $i_t = -\frac{3^\circ}{4}$ ; slats extended;  $\delta_f = 50^\circ$ .